Functional screen identifies regulators of murine hematopoietic stem cell repopulation

Per Holmfeldt,[1]* Miguel Ganuza,[1]* Himangi Marathe,[1] Bing He,[5] Trent Hall,[1] Guolian Kang,[2] Joseph Moen,[2] Jennifer Pardieck,[1] Angelica C. Saulsberry,[1] Alba Cico,[1] Ludovic Gaut,[1] Daniel McGoldrick,[3] David Finkelstein,[3] Kai Tan,[4] and Shannon McKinney-Freeman[1]

[1]Department of Hematology, [2]Department of Biostatistics, and [3]Department of Computational Biology, St. Jude Children's Research Hospital, Memphis, TN 38105
[4]Department of Internal Medicine and [5]Interdisciplinary Graduate Program in Genetics, University of Iowa, Iowa City, IA 52242

Understanding the molecular regulation of hematopoietic stem and progenitor cell (HSPC) engraftment is paramount to improving transplant outcomes. To discover novel regulators of HSPC repopulation, we transplanted >1,300 mice with shRNA-transduced HSPCs within 24 h of isolation and transduction to focus on detecting genes regulating repopulation. We identified 17 regulators of HSPC repopulation: *Arhgef5*, *Armcx1*, *Cadps2*, *Crispld1*, *Emcn*, *Foxa3*, *Fstl1*, *Glis2*, *Gprasp2*, *Gpr56*, *Myct1*, *Nbea*, *P2ry14*, *Smarca2*, *Sox4*, *Stat4*, and *Zfp521*. Knockdown of each of these genes yielded a loss of function, except in the cases of *Armcx1* and *Gprasp2*, whose loss enhanced hematopoietic stem cell (HSC) repopulation. The discovery of multiple genes regulating vesicular trafficking, cell surface receptor turnover, and secretion of extracellular matrix components suggests active cross talk between HSCs and the niche and that HSCs may actively condition the niche to promote engraftment. We validated that *Foxa3* is required for HSC repopulating activity, as *Foxa3*$^{-/-}$ HSC fails to repopulate ablated hosts efficiently, implicating for the first time *Foxa* genes as regulators of HSPCs. We further show that *Foxa3* likely regulates the HSC response to hematologic stress. Each gene discovered here offers a window into the novel processes that regulate stable HSPC engraftment into an ablated host.

Hematopoietic stem cells (HSCs) can reconstitute the entire hematopoietic system after transplantation into hosts whose hematopoietic compartment has been ablated. This is clinically exploited as HSC transplantation (HSCT) to treat hematologic disease and represents the only curative therapy for many disorders (Cavazzana et al., 2014; Cohen et al., 2015; Talano and Cairo, 2015). Unfortunately, the application of HSCT can be limited by a paucity of HSCs, especially in cord blood transplantation (Zhong et al., 2010). As such, tremendous effort has been exerted to develop protocols that allow for the expansion of transplantable HSCs ex vivo. Strategies range from identifying transcriptional regulators and developing supportive stroma to identifying small molecules that promote expansion (Walasek et al., 2012). However, these approaches are limited by the tendency of HSCs to differentiate in culture and have not yet been clinically translated.

One alternative for improving HSCT is to enhance HSC engraftment itself. Successful HSCT requires that donor HSCs engage with the proper supporting niche, survive, proliferate, and differentiate into mature blood lineages. These processes are associated with numerous stresses, including myelotoxic conditioning that alters the niche, ex vivo manipulation of HSCs, and the requirement for supraphysiological hematopoietic expansion during engraftment and reconstitution. Recent studies indicate that stress hematopoiesis, including that which occurs after HSCT, is subject to distinct biological regulation compared with baseline hematopoiesis occurring in healthy individuals (Rossi et al., 2012). Further, the hematopoietic stem and progenitor cells (HSPCs) that maintain hematopoiesis after HSCT may differ from those that sustain native hematopoiesis (Sun et al., 2014; Busch et al., 2015). These differences highlight the importance of dissecting the cellular and molecular mechanisms that uniquely regulate the function of HSPCs after transplant. PGE2, shown to promote HSC engraftment by up-regulating homing pathways and enhancing self-renewal has recently been tested in Phase 1 clinical trials where it enhanced the long-term engraftment of cord blood (Hoggatt et al., 2009; Cutler et al., 2013). Although more work is needed, this suggests that enhancing HSC engraftment can improve transplant outcomes. Understanding the mechanisms that regulate the stable repopulation of the hematopoietic compartment by HSPCs is paramount to developing new therapies to further improve

*P. Holmfeldt and M. Ganuza contributed equally to this paper.

Correspondence to Shannon McKinney-Freeman: shannon.mckinney-freeman@stjude.org

Abbreviations used: DCFDA, 2′,7′-dichlorofluorescein diacetate; HSC, hematopoietic stem cell; HSCT, HSC transplantation; HSPC, hematopoietic stem and progenitor cell; IM-PET, integrated method for predicting enhancer targets; LDA, limiting dilution analysis; LSK, Lineage$^-$Sca-1$^+$c-Kit$^+$; MPP, multipotent progenitor; PB, peripheral blood; qRT-PCR, quantitative RT-PCR; ROS, reactive oxygen species; TBHP, tert-Butyl hydrogen peroxide; WBM, whole BM.

The Rockefeller University Press $30.00
J. Exp. Med. 2016 Vol. 213 No. 3 433–449
www.jem.org/cgi/doi/10.1084/jem.20150806

The Journal of Experimental Medicine

HSCT. Thus, here we report a functional screen for novel regulators of HSPC engraftment and repopulation.

Prior functional screens of murine and human HSCs have focused on identifying genes that promote HSPC self-renewal and/or maintenance during ex vivo culture (Ali et al., 2009; Deneault et al., 2009; Boitano et al., 2010; Hope et al., 2010; Fares et al., 2014). In these studies, purified murine HSCs or enriched human HSPCs were transduced with the open reading frames of genes of interest (GOI), transduced with shRNAs targeting GOI, or treated with small molecule libraries. Cells were then maintained ex vivo for 5–17 d before downstream assays, which included transplantation into ablated mice for a rigorous functional assessment of HSC numbers, in vitro colony assays, or flow cytometry for retention of an HSPC cell surface phenotype. In each of these studies, extensive ex vivo culture before downstream analysis precluded a direct assessment of the effect of treatment on HSC engraftment, as this would be difficult to separate from effects on HSC expansion, differentiation during culture, or even non–cell-autonomous effects on HSC maintenance, as was seen in one study (Deneault et al., 2009). In contrast, our goal is to identify genes critically required for the stable repopulation of an ablated hematopoietic system. To achieve this, we developed a system in which HSPCs treated with shRNAs are subjected to minimal ex vivo culture before transplantation into cohorts of ablated mice, allowing us to directly assess any effect of the loss of gene expression on HSC engraftment and hematopoietic reconstitution. Here, we report the identification of 17 genes whose loss perturbs short- and long-term HSPC repopulation: 15 genes required for optimal repopulation and 2 inhibitors of stable HSPC engraftment, as their loss enhanced HSPC repopulation. 12 of these genes have never before been implicated in HSPC biology, including *Foxa3* (formally known as hepatocyte nuclear factor 3γ or HNF-3γ). *Foxa3* belongs to the *Foxa* subclass of *Fox* (Forkhead Box) DNA-binding factors. FOXA proteins are transcriptional pioneer factors that establish competence for downstream transcriptional programs (Friedman and Kaestner, 2006). *Foxa3* has primarily been studied for its role in endoderm and endoderm-derived tissue development (Friedman and Kaestner, 2006). However, a role for *Foxa3* in several nonendodermal lineages has recently been described (Behr et al., 2007; Ionescu et al., 2012; Xu et al., 2013), suggesting a broader role in tissue development and function. Here, we further demonstrate a novel role for *Foxa* genes in HSC biology via investigation of *Foxa3*$^{-/-}$ mice.

RESULTS

Identification of candidate genes for functional screen

The following public databases of HSC gene expression were interrogated to prioritize 51 gene candidates for study: Hematopoietic Fingerprints, the Immunological Genome Project, and StemSite (Chambers et al., 2007; Heng and Painter, 2008; McKinney-Freeman et al., 2012). Gene candidates were prioritized if their expression was enriched in adult HSC relative to downstream progeny or earlier stages of HSC ontogeny. Quantitative RT-PCR (qRT-PCR) was used to interrogate the expression of each prioritized gene candidate in cells isolated from murine BM (Fig. 1, A and B). We found that 44/51 GOI were expressed in lineage$^-$ BM hematopoietic cells, the majority of which were highly enriched for expression in Lineage$^-$Sca-1$^+$c-Kit$^+$ (LSK) cells relative to downstream progeny (Fig. 1 B).

To interrogate a role for GOI in HSC engraftment, we used shRNAs to disrupt their expression in LSK cells before transplantation into lethally irradiated mice. At least four miR-30–embedded shRNAs were designed to target each of the 44 GOI whose expression was validated in HSPCs. shRNAs were cloned into a lentiviral vector downstream of an MSCV promoter and upstream of a phosphoglycerate kinase promoter driving the fluorescent reporter mCherry (Fig. 1 A). Each shRNA was transduced into LSK cells and tested for gene knockdown by qRT-PCR. Mean transduction for these experiments was 76.7 ± 7% (Fig. 1 C). At least two shRNA were identified that affected >75% transcript knockdown in LSK cells for 41/44 GOI (Fig. 1 D and Table S2). Thus, these genes were further screened.

We next conducted pilot studies to assess the feasibility of using highly purified HSCs (LSK CD150$^+$CD48$^-$ cells) in our screen. CD45.2$^+$ HSCs were transduced with control shRNAs and transplanted with an equal number of mock-transduced CD45.1$^+$ HSCs into CD45.1$^+$/CD45.2$^+$ recipients. These experiments suffered from high signal/noise incompatible with a robust screen (unpublished data). We determined that this high signal/noise resulted primarily from the technical difficulty of evenly distributing small cell numbers among mice in a cohort. Thus, we chose to use the more abundant LSK cell population for our screen. Although LSK cells are a mixture of HSPCs, by >16 wk after transplants, we can readily assess the effect of gene knockdown on stable HSC repopulation. Indeed, pilot studies also revealed that HSCs consistently transduce with a slightly higher frequency than LSK cells (Fig. 1 E). Thus, HSCs are robustly transduced in our system.

Functional screen for novel regulators of HSC engraftment

CD45.2$^+$ Test LSK cells were transduced with individual shRNAs and then transplanted into ablated CD45.1$^+$/CD45.2$^+$ mice with an equal number of CD45.1$^+$ mock-transduced Competitor LSK cells (Fig. 2 A). Cells were transplanted within 24 h of their isolation and transduction; i.e., there was no extended ex vivo culture period as in previous functional screens of primary HSPCs (Ali et al., 2009; Deneault et al., 2009; Hope et al., 2010). For each transplant, an aliquot of transduced cells was maintained in liquid culture and analyzed after 3–4 d for transduction efficiency. Mean transduction for these experiments was 67.6 ± 8.5% (Fig. 2 B). Recipient peripheral blood (PB) was analyzed for Test versus Competitor contribution for >16 wk after transplant. A total of 781 mice were transplanted.

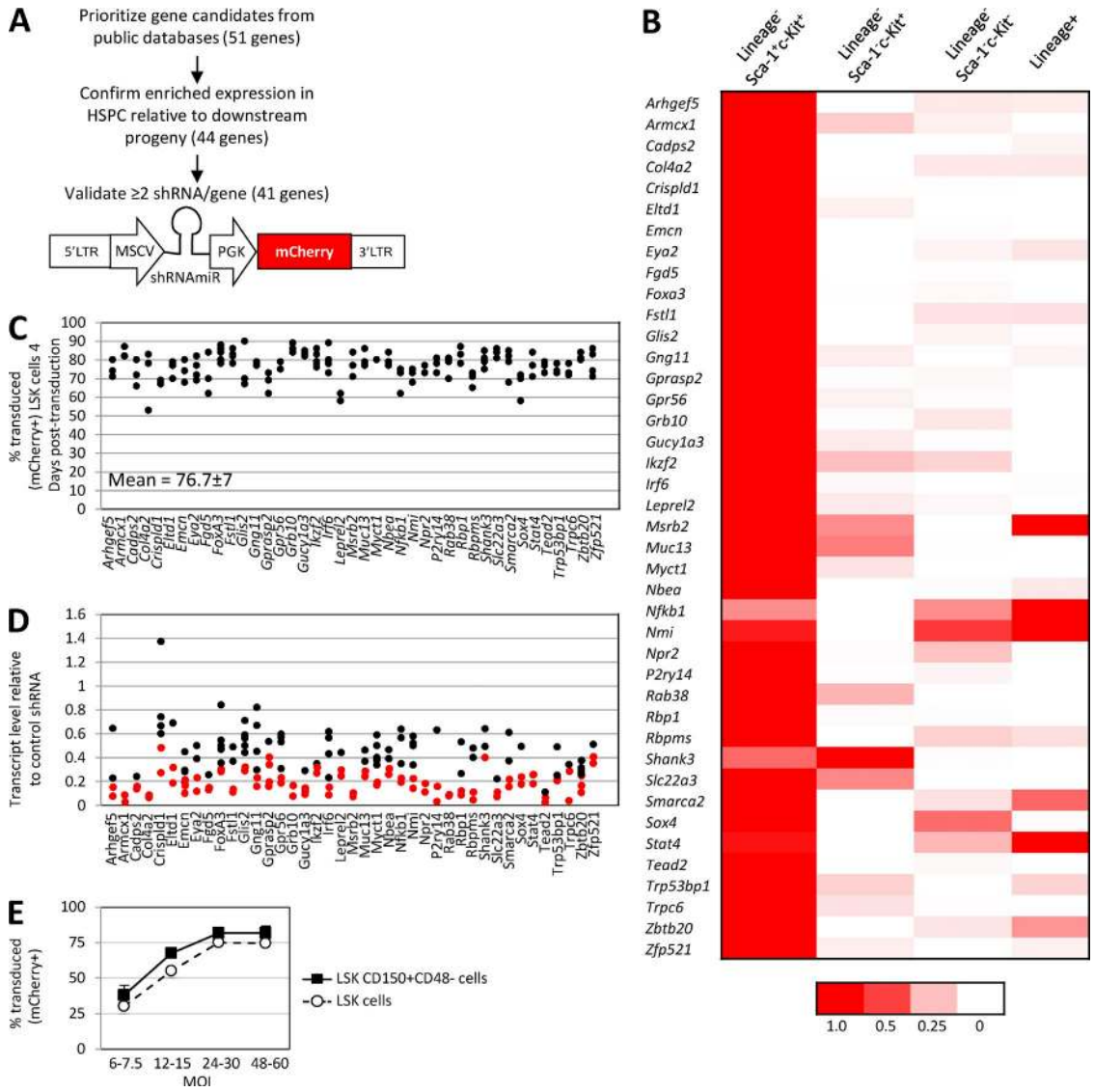

Figure 1. **Functional screen for regulators of HSPC in vivo repopulation.** (A) Screen schematic. 51 prioritized genes were assessed by qRT-PCR for expression in LSK cells. miR30-embedded shRNAs targeting each gene expressed in LSK cells were cloned into a lentiviral vector downstream of the MSCV promoter. Here, the phosphoglycerate kinase (PGK) promoter drives mCherry. (B) Heat map of qRT-PCR of GOI in LSK cells, Lineage$^-$ cells, and Lineage$^+$ cells. Scale indicates gene expression relative to population expressing the highest level of each gene across each row (1 = dark red). (C) BM LSK cells transduced with shRNAs were assayed 3–4 d after transduction for mCherry. Each circle is an independent transduction event. (D) BM LSK cells transduced with shRNAs were examined 3–4 d after transduction by qRT-PCR. Each circle is an independently screened shRNA. Circles in red denote shRNAs used in the screen. (E) Transduction efficiency (%mCherry$^+$) of LSK cells and HSCs (i.e., LSK CD150$^+$CD48$^-$) at multiple MOI 4 d after transduction.

Loss-of-function hits

Knockdown of 18 genes resulted in a loss of HSPC repopulating potential relative to control with two independent shRNAs in our initial screen (*Arhgef5*, *Cadps2*, *Col4a2*, *Crispld1*, *Emcn*, *Foxa3*, *Glis2*, *Gng11*, *Gpr56*, *Myct1*, *Nbea*, *P2ry14*, *Rbpms*, *Sox4*, *Stat4*, *Trp53bp1*, *Trpc6*, and *Zbtb20*; Fig. 2 C). Repopulation loss was apparent 4 wk after transplant and persisted for >16 wk for all GOI except *Stat4* (Fig. 2 C), where the loss of repopulation was most dramatic >16 wk after transplant. Knockdown of most of these genes did not affect the short-term (i.e., 14 d) maintenance of hematopoietic cells ex vivo (unpublished data). In contrast, knockdown of 20 GOI did not affect in vivo repopulating potential (Fig. 2 D). To confirm stable gene knockdown in our system, mice transplanted with LSK cells transduced with *Grb10* shRNAs, a non-hit, were examined (Fig. 2, E–G). Both *Grb10* shRNAs effected >95% transcript loss in LSK cells (Fig. 2 F). qRT-PCR analysis of CD45.2$^+$ LSK cells isolated from mice transplanted 30 wk prior with either control or *Grb10* shRNA–treated cells revealed persistent gene knockdown in these cells (Fig. 2 G).

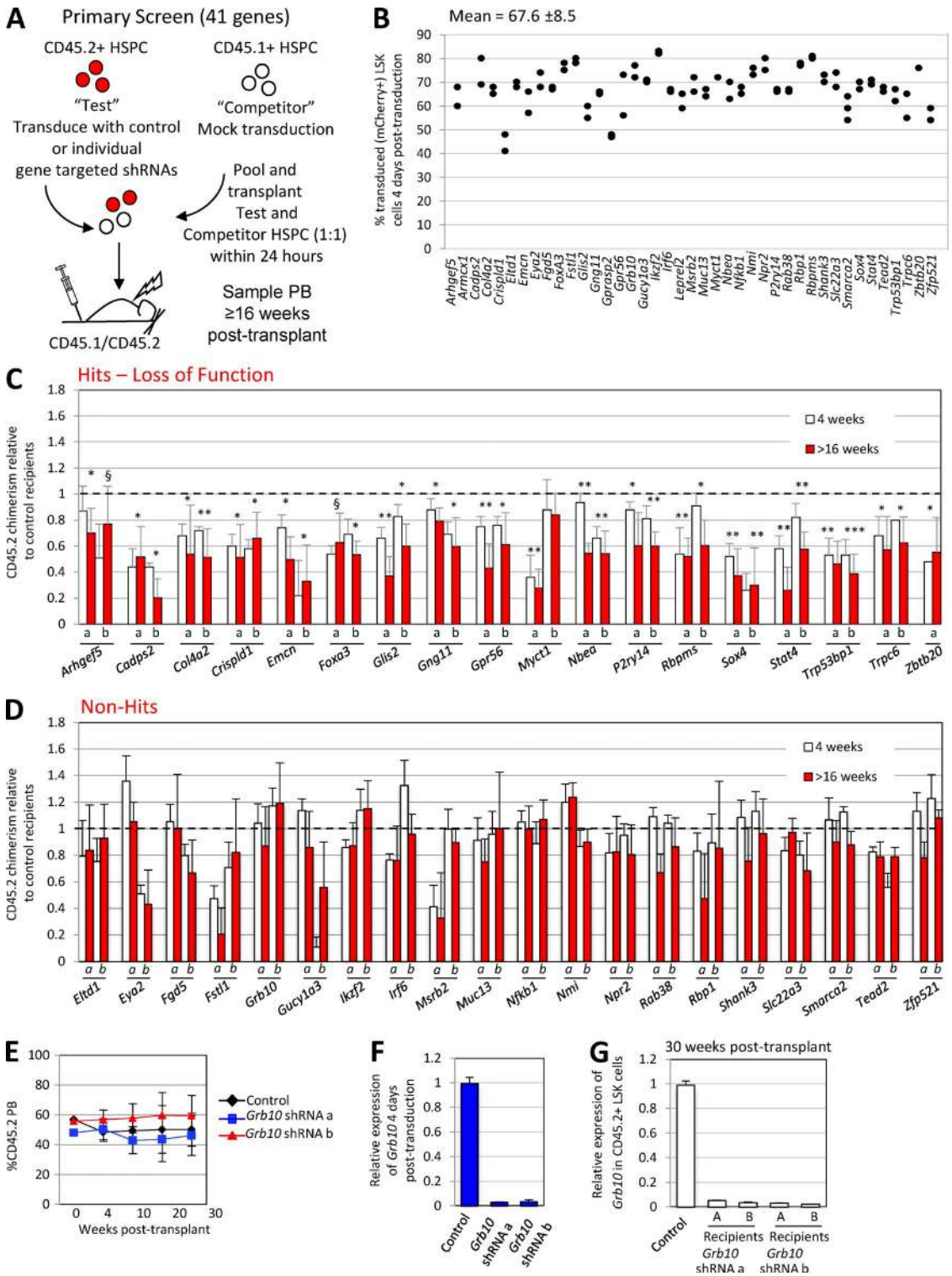

Figure 2. **Identification of genes required for HSPC in vivo repopulation.** (A) shRNAs were transduced into CD45.2$^+$ Test LSK cells that were then transplanted into CD45.1$^+$/CD45.2$^+$ mice with an equal number of CD45.1$^+$ mock-transduced Competitor LSK cells. Recipient PB was analyzed for >16 wk for CD45.2$^+$ cells. (B) Transduction of Test LSK cells for each screen transplant. For each transplant, an aliquot of Test cells was assessed for the percentage of mCherry$^+$ cells 4 d after transduction. Each circle represents an independent transduction. (C and D) Loss-of-function hits (C) and non-hits (D). Percentage of CD45.2 PB 4 and >16 wk after transplant of recipients of gene-specific shRNA–treated Test cells normalized to that of recipients of control shRNA–treated Test cells. Each gene was interrogated with two independent shRNAs (labeled as a and b). (E) Percentage of CD45.2 PB of mice transplanted with

Knockdown of six GOI yielded a repopulating loss with only 1/2 shRNAs tested (*Eya2*, *Fstl1*, *Gucy1a3*, *Msrb2*, *Rbp1*, and *Myct1*; Fig. 2, C and D). In each case, except *Myct1* (discussed in the next section), this loss of repopulation was attributable to nonspecific toxicity of the effecting shRNA (e.g., a third *Gucy1a3* shRNA did not affect repopulation; Fig. 3 F).

Confirmation of loss-of-function screen hits

The 18 hits identified in our screen were retested to confirm their role as regulators of LSK cell in vivo repopulating activity. Here, to improve resolution, only vector$^+$ Test LSK cells (mCherry$^+$CD45.2$^+$) were transplanted into ablated mice (Fig. 3 A). Cells were sorted and transplanted 44 h after transduction, along with an equal number of CD45.1$^+$ mock-transduced and mock-sorted Competitor LSK cells. A series of pilot studies revealed that a minimum of 40 h was required after transduction to visualize and isolate vector$^+$ LSK cells by flow cytometry (Fig. 3 B). Here, we also retested five genes that scored as non-hits (*Fstl1*, *Gucy1a3*, *Rbp1*, *Smarca2*, and *Zfp521*; Fig. 2 D). *Smarca2* and *Zfp521* were retested because transduction efficiency was low in our initial screen for these genes or their shRNAs did not yield a complete gene knockdown, resulting in a possible false negative (Fig. 3, C and D). *Fstl1*, *Gucy1a3*, and *Rbp1* were non-hits whose two shRNAs yielded disparate outcomes in our initial screen, necessitating a more thorough analysis. A total of 527 mice were transplanted in these experiments.

15 loss-of-function hits retested were confirmed as requirements for optimal HSPC repopulation (Fig. 3 E). Repopulation loss was more dramatic in these experiments relative to our initial screen, likely because of greater resolution resulting from transplantation of only vector$^+$ cells. Three genes that initially scored as non-hits were scored as hits when retested: *Fstl1*, *Smarca2*, and *Zfp521*. As mentioned, the transduction efficiencies for *Smarca2* and *Zfp521* were low in our initial screen (Fig. 3 C), likely resulting in a false negative in those experiments. As both transduction and gene knockdown for *Fstl1* were high in our initial screen (Fig. 2 B and not depicted), it appears that transplantation of only vector$^+$ cells is necessary to clearly resolve a repopulating loss with both *Fstl1* shRNAs. Alternatively, the prolonged culture in these experiments might exact additional stress on the cells, resulting in a loss of in vivo repopulation not apparent in our original screen. Six initial hits did not affect repopulating potential when retested: *Col4a2*, *Gng11*, *Rbpms*, *Trp53bp1*, *Trpc6*, and *Zbtb20* (Fig. 3 F). As only one *Zbtb20* shRNA was tested in our initial screen, two additional *Zbtb20* shRNAs were tested in our confirmation experiments (Fig. 3 F). Only the original *Zbtb20* shRNA mediated a loss of repopulation, suggesting that this shRNA likely had off-target effects. Once again, *Stat4* was the only hit that displayed a significant increase in repopulating loss between 4 and >16 wk after transplant (Fig. 3 E), suggesting that *Stat4* regulates the long-term repopulating potential of HSCs, rather than their early engraftment. The distribution of T, B, or myeloid cells in the mCherry$^+$CD45.2$^+$ compartment of recipients was only significantly perturbed in recipients of *Cadps2* and *Foxa3* shRNA–treated cells (Fig. 3 G). Loss of *Cadps2* resulted in a significant expansion of B cells and a concomitant loss of T cells, suggesting that lymphoid progenitor function might be perturbed. Loss of *Foxa3* perturbed the myeloid compartment (Fig. 3 G).

In sum, via our two-pronged screening approach, we rigorously identified 15 genes required for LSK cell in vivo repopulating activity: *Arhgef5*, *Cadps2*, *Crispld1*, *Emcn*, *Foxa3*, *Fstl1*, *Glis2*, *Gpr56*, *Myct1*, *Nbea*, *P2ry14*, *Smarca2*, *Sox4*, *Stat4*, and *Zfp521* (Fig. 3 E). These GOI regulate a diverse array of cellular processes, including epigenetics, adhesion and migration, vesicle trafficking and cell surface receptor turnover, and the extracellular matrix.

Gain-of-function hits: loss of *Gprasp2* and *Armcx1* promotes HSPC repopulation

Loss of *Gprasp2* appeared to favor LSK cell in vivo repopulating activity in our study. Here, mCherry$^+$CD45.2$^+$ was positively selectedover time in the PB of 17/20 recipients of *Gprasp2* shRNA–transduced LSK cells compared with only 2/9 recipients of control cells (Fig. 4 A). Similarly, loss of *Armcx1* also appeared to enhance HSPC repopulation (Fig. 4 Bi). As only mCherry$^+$ cells were transplanted in these experiments, it was not possible to monitor for mCherry selection. However, although not statistically significant, 7/11 recipients of *Armcx1* shRNA–transduced Test HSPCs showed moderately enhanced chimerism >16 wk after transplant relative to controls (Fig. 4 B, i). To rigorously assess whether loss of *Armcx1* or *Gprasp2* enhanced LSK cell in vivo repopulating activity, mCherry$^+$CD45.2$^+$ Test LSK cells (transduced with either gene-specific or control shRNAs) were transplanted 1:4 with CD45.1$^+$ mock-transduced and mock-sorted Competitor LSK cells, thus putting the Test cells at a significant repopulating disadvantage relative to Competitor. Here, loss of *Armcx1*

Grb10 shRNA or control shRNA–transduced Test cells. Knockdown of *Grb10* had no effect on LSK cell repopulating activity. (F) LSK cells transduced with control or *Grb10* shRNAs were examined 4 d after transduction for the percentage of mCherry$^+$ cells. (G) 30 wk after transplant, CD45.2$^+$ LSK cells were isolated from the BM of individual mice transplanted with CD45.2$^+$ LSK cells transduced with either control or *Grb10* shRNAs. These cells were examined by qRT-PCR for *Grb10* transcript levels. For C–F, the mean of five recipient mice is presented, and error bars represent SD. For C, a one-sample Student's *t* test was performed testing the null hypothesis that the normalized measurements = 1. P-values are two-sided. §, $P < 0.1$; *, $P < 0.05$; **, $P < 0.005$; ***, $P < 0.0001$. Only p-values calculated >16 wk after transplant are shown.

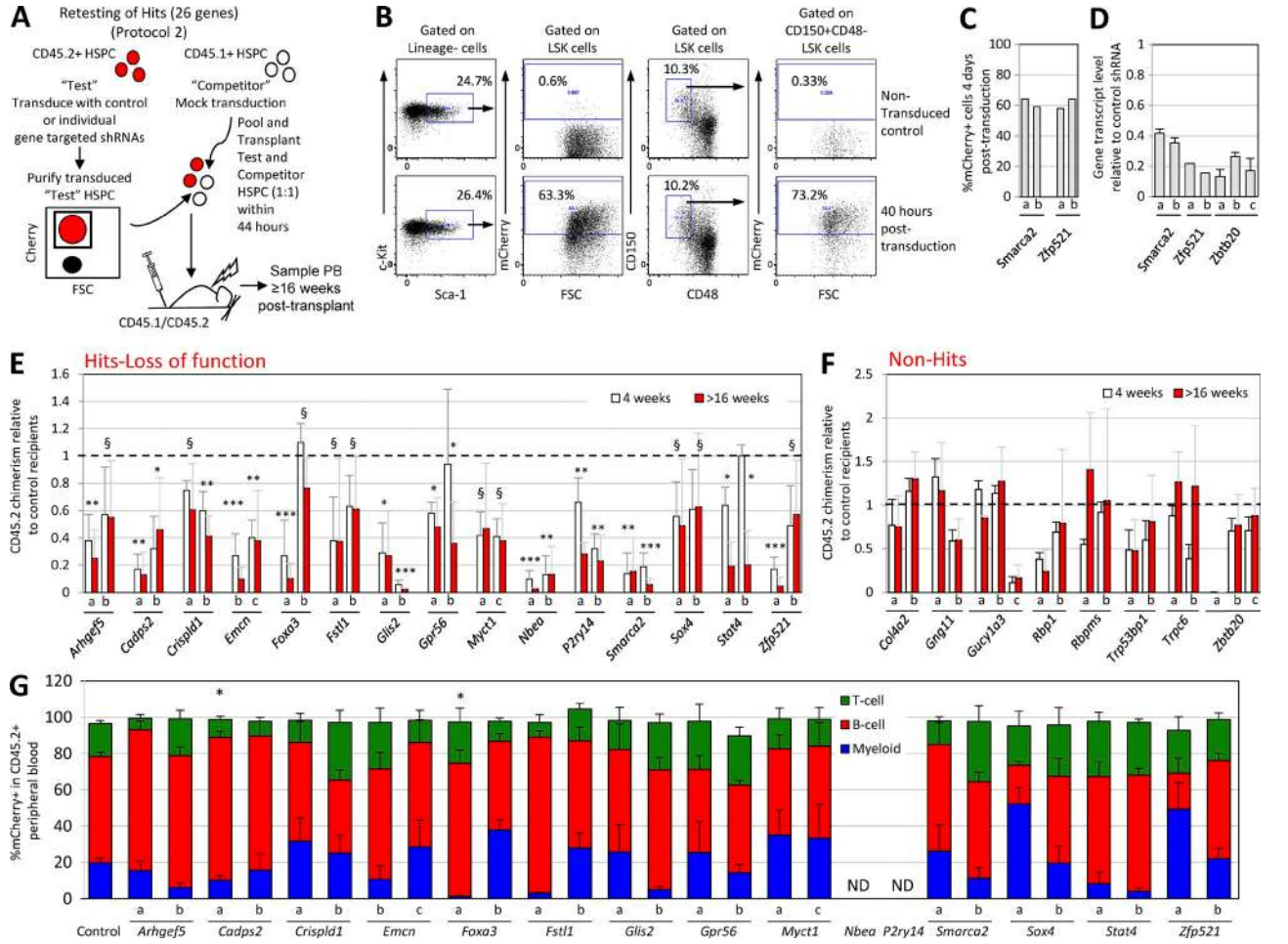

Figure 3. **Validation of loss-of-function hits identifies 15 genes required for robust HSPC repopulating activity.** (A) For retesting hits, mCherry$^+$CD45.2$^+$ Test HSPCs (LSK cells) transduced with either control or gene-specific shRNAs were transplanted into CD45.1$^+$/CD45.2$^+$ mice with an equal number of CD45.1$^+$ mock-transduced and mock-sorted Competitor HSPCs. Recipient PB was analyzed for >16 wk for CD45.2$^+$ cells. (B) Representative flow cytometry analysis of LSK cell and HSCs (i.e., LSK CD150$^+$CD48$^-$) 40 h after transduction with control shRNA lentiviral vector. Samples were examined for the frequency of mCherry$^+$ cells. (C) Transduction efficiency (percentage of mCherry$^+$ cells) of Test LSK cells transduced with *Smarca2* and *Zfp521* shRNAs in primary screen. (D) Knockdown efficacy of shRNAs targeting *Smarca2*, *Zfp521*, and *Zbtb20* assessed by qRT-PCR 3–4 d after transduction of LSK cells. (E) Verified loss-of-function hits. A one sample Student's *t* test was performed testing the null hypothesis that the normalized measurements = 1. P-values are two-sided. §, $P < 0.1$; *, $P < 0.05$; **, $P < 0.005$; ***, $P < 0.0001$. Only p-values calculated >16 wk after transplant are shown. (F) Functional screen non-hits. In E and F, each gene was interrogated with at least two independent shRNAs (labeled as a, b, or c) and the percentage of CD45.2 PB at 4 and >16 wk after transplant of recipients of gene-specific shRNA–treated Test cells normalized to that of recipients of control shRNA–treated Test cells is shown. (G) Distribution of T, B, and myeloid PB lineages in mCherry$^+$CD45.2$^+$ compartment of genes that scored as hits after retesting >16 wk after transplant. In E–G, each bar is the average of at least four recipient mice, and error bars represent SD. In G, asterisks denote a statistically significant difference in distribution of at least one lineage relative to control for both shRNAs tested ($P < 0.05$). P-values were calculated using the exact Wilcoxon Mann-Whitney test. ND, not determined.

and *Gprasp2* enhanced the repopulating potential of Test LSK cells in the majority of transplanted mice (Fig. 4 B, ii). This result was true for multiple independent shRNAs tested for each gene. Loss of *Armcx1* and *Gprasp2* did not appear to perturb any specific hematopoietic PB lineages (Fig. 4 C). Loss of the gene *Leprel2* also appeared to enhance repopulation in both our initial screen and after retesting ($P = 0.02$; Fig. 4 B, i; and not depicted). However, when *Leprel2* was reexamined in a 1:4 Test versus Competitor transplant, enhanced repopulation was no longer apparent (Fig. 4 B, ii).

In summary, loss of *Gprasp2* and *Armcx1* enhanced LSK cell repopulating activity, suggesting that these genes may negatively impact HSPC engraftment. Interestingly, *Gprasp2* and *Armcx1* belong to the same family of G-protein coupled receptor associated sorting proteins (GASP), strongly implicating this gene family in the negative regulation of HSPC repopulating potential (Abu-Helo and Simonin, 2010).

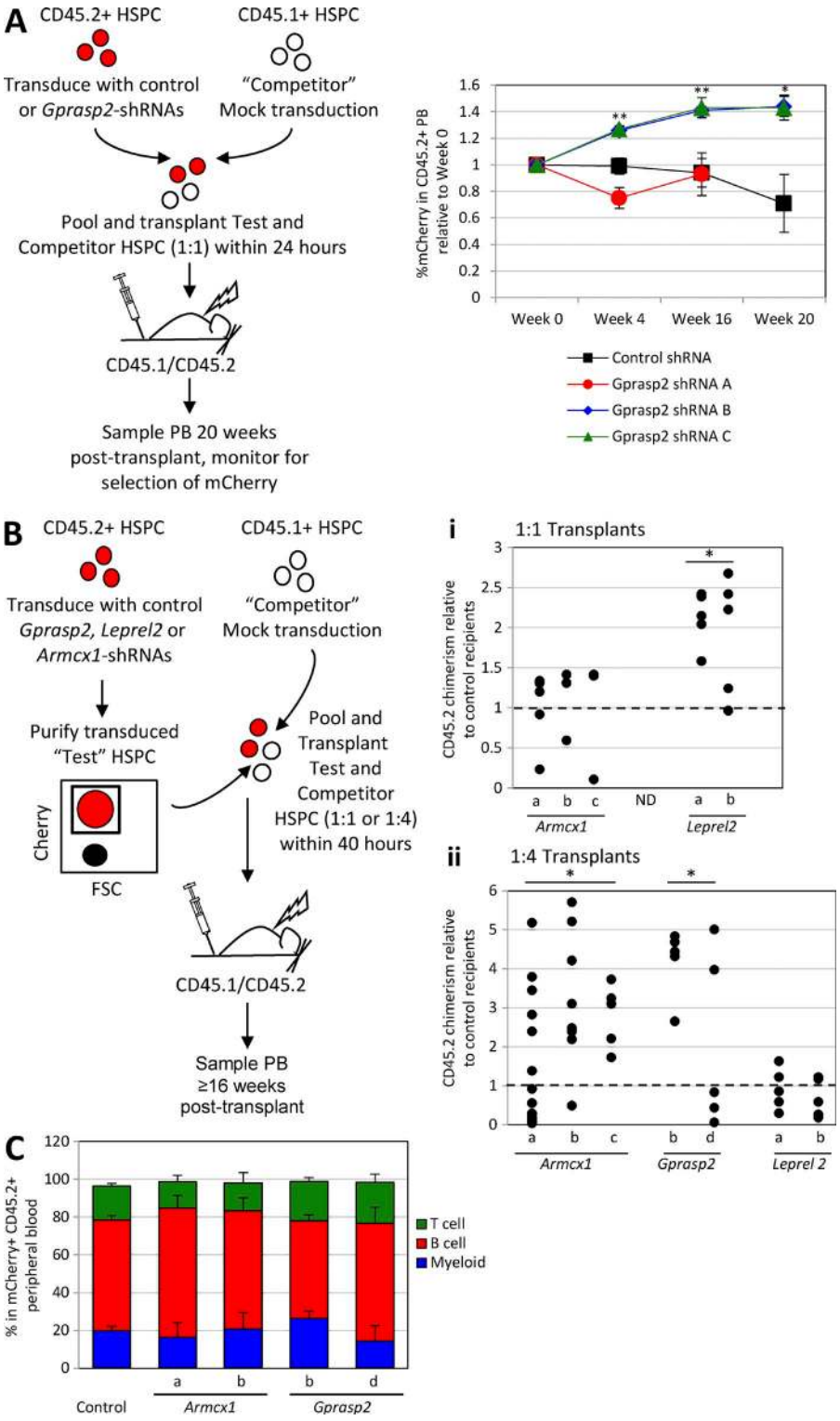

Figure 4. **Functional screen identifies *Gprasp2* and *Armcx1* as negative regulators of HSPC repopulation.** (A) *Gprasp2* or control shRNAs were transduced into CD45.2$^+$ LSK cells that were then transplanted into CD45.1$^+$/CD45.2$^+$ mice with an equal number of CD45.1$^+$ mock-transduced Competitor LSK cells. Recipient PB was analyzed for 20 wk. Percentage of mCherry$^+$ CD45.2$^+$ PB of recipients of *Gprasp2* shRNA–treated cells normalized to the percentage of mCherry$^+$CD45.2$^+$ PB of recipients of control shRNA–treated cells. *Gprasp2* was tested in two independent experiments with three shRNAs (a–c). Cumulative results shown for both experiments ($n \geq 5$ at all time points). (B) Validation of gain-of-function hits (*Gprasp2*, *Armcx1*, and *Leprel2*). *Gprasp2*, *Leprel2*, *Armcx1*, or control shRNAs were transduced into CD45.2$^+$ HSPCs. mCherry$^+$ HSPCs were resorted 40 h after transfection and transplanted either 1:1 or 1:4 with CD45.1$^+$ mock-transduced and mock-sorted Competitor HSPCs into CD45.1$^+$/CD45.2$^+$ mice. Data shown is the percentage of CD45.2$^+$ recipient PB of gene-specific shRNA–treated cells normalized to that of recipients of control shRNA–treated cells at >16 wk after transplant for 1:1 (i) or 1:4 (ii) transplants. *Armcx1* was examined with three shRNAs (a–c) in a single (i) and three (ii) independent experiments. *Gprasp2* was interrogated with two shRNAs (b and d) in a single experiment (ii). *Leprel2* was examined with two shRNAs (a and b) in a single experiment for both i and ii. (C) Distribution of T, B, and myeloid PB lineages in mCherry$^+$CD45.2$^+$ compartment of gain-of-function hits from >16 wk after transplant. In A and C, each value is the mean of $n \geq 5$ mice; error bars represent SD. *, $P < 0.04$; **, $P < 0.008$. P-values were calculated via exact Wilcoxon Mann-Whitney test.

Interrogation of the cellular mechanism of gene loss on HSPC repopulating potential

To illuminate the cellular mechanisms of gene knockdown on HSPCs, LSK cells transduced with control or gene-specific shRNAs were assayed for CFU potential, cell cycle, and apoptosis (Fig. 5, A and B; and Fig. S1). We also examined CD45.2$^+$ chimerism in the BM of recipients of gene-deficient CD45.2$^+$ LSK cells >16 wk after transplant (Fig. 5 C).

LSK cells lacking *Nbea* and *Glis2* displayed an increase in CFU-GEMM potential ($P = 0.046$ and 0.07, respectively;

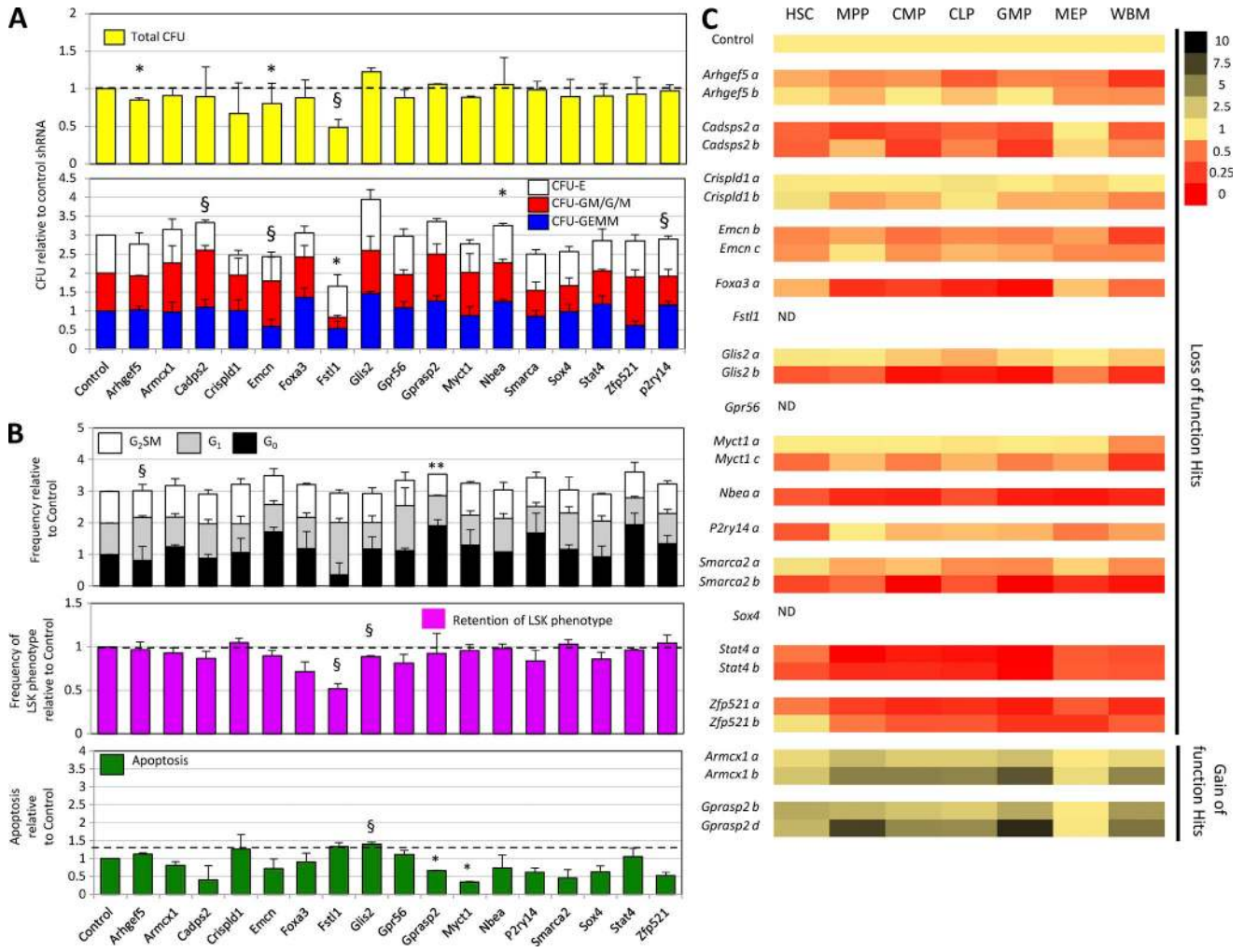

Figure 5. **Functional analysis of screen hits.** (A) 500 mCherry$^+$ LSK cells transduced with control or gene-specific shRNAs were assayed for CFU potential 5 d after transduction. Values are the mean of two to three independent experiments normalized to control ± SE. (B) Cell cycle status of the mCherry$^+$ LSK cell compartment, the frequency of mCherry$^+$ LSK cells, and apoptosis of mCherry$^+$ LSK cells was analyzed 5 d after transduction with control or gene-specific shRNAs. Values are the mean of two to three independent experiments normalized to control ± SE. For A and B, a one-sample Student's *t* test was performed testing the null hypothesis that the normalized measurements = 1. P-values are two-sided. §, $P < 0.1$; *, $P < 0.05$; **, $P < 0.005$. (C) Heat map summarizing mean percentage of CD45.2$^+$ (Test cell–derived) HSC, MPP, CMP, CLP, GMP, and MEP in recipients >16 wk after transplant. Values are normalized to control recipients (i.e., 1 = yellow). Higher chimerism relative to control = darker green; lower chimerism relative to control = darker red. ND, not determined.

Fig. 5 A). This correlated with a loss of CD45.2$^+$ chimerism downstream of HSCs or multipotent progenitors (MPPs) in recipients of LSK cells deficient in these genes (Fig. 5 C). These data suggest a block in differentiation at the HSC or MPP stage, resulting in an accumulation of CFU-GEMM. *Glis2*-deficient LSK cells also displayed elevated apoptosis ex vivo ($P = 0.08$; Fig. 5 B), suggesting that this block in differentiation exists in concert with reduced progenitor survival downstream of HSCs and MPPs.

Knockdown of *Stat4*, *Zfp521*, and *Foxa3* also resulted in an enhanced loss of CD45.2$^+$ chimerism downstream of HSCs in transplanted mice (Fig. 5 C). Knockdown of *Zfp521* in LSK cells ex vivo resulted in a slight expansion of CFU-G/M/GM at the expense of CFU-GEMM ($P = 0.08$) and an ∼50% loss of apoptotic cells, although CFU-G/M/GM expansion and loss of apoptosis did not score as statistically significant here (Fig. 5, A and B). These data suggest that CFU-GEMM lacking *Zfp521* differentiate rapidly to committed progenitors that display enhanced survival ex vivo, but fail to establish robust chimerism in vivo.

Arhgef5 and *Emcn* knockdown caused a significant loss in total CFU from LSK cells ($P = 0.027$; $P = 0.035$, respectively), whereas *Fstl1* knockdown resulted in a dramatic, but only marginally significant, loss in CFU ($P = 0.096$; Fig. 5 A). This correlated with a loss of CD45.2$^+$ chimerism across all BM compartments in recipients of LSK cells deficient in these genes, except for *Fstl1*, for whom BM chimerism was not determined (Fig. 5 C). As *Emcn*-deficient LSK cells did not dis-

play significant perturbations in cell cycle or apoptosis ex vivo, loss of in vivo repopulating activity may result from perturbed niche interactions after transplant effecting survival, differentiation, or proliferation. However, *Arhgef5*-deficient LSK cells displayed about a 40% expansion of cells in G_1 ex vivo, relative to control ($P = 0.089$), which was commensurate with a modest reduction of cells in both G_0 and G_2–S–M ($P > 0.05$ for both). Thus, perturbations in cell cycle progression may contribute to the repopulating defect of *Arhgef5*-deficient LSK cells. In addition to a dramatic loss in total CFU, *Fstl1*-deficient cells displayed a rapid loss of the LSK cell surface phenotype during culture ($P = 0.079$), suggesting accelerated differentiation commensurate with a loss of stem and progenitor cell potential. Knockdown of *Cadps2* in CD45.2$^+$ LSK cells also resulted in a loss of CD45.2$^+$ chimerism across all BM compartments after transplant (Fig. 5 C). This correlated with perturbations in the frequency of select CFU: a marginally significant, albeit modest, loss of CFU-E ($P = 0.057$) and a marginally significant increase in CFU-G/M/GM ($P = 0.06$) was apparent after knockdown of this gene (Fig. 5 A).

In contrast, recipients of *Armcx1* and *Gprasp2* shRNA–treated cells displayed enhanced CD45.2$^+$ chimerism in all HSPC compartments, correlating with enhanced PB chimerism (Fig. 4 B and Fig. 5 C). LSK cells treated with *Gprasp2* shRNAs displayed significantly enhanced survival ex vivo and a twofold expansion of cells in G_0, commensurate with a loss of cells in G_2–S–M ($P = 0.002$). Thus, enhanced survival and a slow-growing phenotype may contribute to enhanced in vivo repopulation here, as observed in *Runx1* mutants whose HSCs also display a repopulating advantage (Cai et al., 2015). In contrast, knockdown of *Armcx1* in LSK cells ex vivo had no significant effect on CFU formation, cell cycle, or apoptosis (Fig. 5, A and B), suggesting that enhanced repopulation after knockdown of *Armcx1* may result from specific in vivo interactions.

Foxa3$^{-/-}$ HSCs display reduced in vitro and in vivo hematopoietic potential

Our screen identified *Foxa3* as a putative novel regulator of LSK cell in vivo repopulating activity (Fig. 2 C and Fig. 3 E). As *Foxa* genes have never been implicated in hematopoiesis, we decided to explore *Foxa3*'s putative role in HSCs further by examining *Foxa3*$^{-/-}$ mice. Although *Foxa3* is selectively expressed by HSCs in BM (Fig. 6 A), *Foxa3*$^{-/-}$ mice display normal PB counts and BM HSPC frequencies (Fig. 6, B and C). *Foxa3*$^{-/-}$ HSCs generated fewer CFU than *Foxa3*$^{+/+}$ HSCs, suggesting a loss of functional HSCs, which could result from fewer absolute numbers of functional HSCs or a failure of HSC activation in culture (Fig. 6 D). Interestingly, *Foxa3*$^{-/-}$ LSK cells showed no loss of CFU potential relative to *Foxa3*$^{+/+}$ LSK cells (unpublished data). As LSK cells are a mix of HSCs and progenitors, these data suggest that progenitors downstream of *Foxa3*$^{-/-}$ HSCs retain CFU potential.

CD45.2$^+$ *Foxa3*$^{-/-}$ or *Foxa3*$^{+/+}$ whole BM (WBM) was transplanted with an equal amount of CD45.1$^+$ WBM into ablated CD45.1$^+$/CD45.2$^+$ recipients (Fig. 6, E and F). A significant loss in CD45.2$^+$ PB reconstitution was apparent in *Foxa3*$^{-/-}$ recipients relative to *Foxa3*$^{+/+}$ recipients 20 wk after transplant (Fig. 6 F). There was no obvious skewing in the reconstitution of specific PB lineages in *Foxa3*$^{-/-}$ recipients (unpublished data). Although *Foxa3*$^{-/-}$ cells contributed less than *Foxa3*$^{+/+}$ cells to recipient LSK, HSC, and MPP compartments (Fig. 6 G), *Foxa3*$^{-/-}$ chimerism in downstream progenitor compartments was unperturbed (unpublished data). When CD45.2$^+$ WBM from primary recipients was transplanted into secondary recipients, *Foxa3*$^{-/-}$ WBM displayed an even more pronounced repopulating defect than in primary transplants (Fig. 6, E and F), suggesting that *Foxa3*$^{-/-}$ HSCs do not self-renew efficiently. Finally, *Foxa3*$^{-/-}$ WBM contained significantly fewer repopulating HSCs, relative to control, when transplanted at limiting dilutions (Fig. 6 H and Table S3; $P = 0.0046$).

In sum, *Foxa3*$^{-/-}$ HSCs are defective in CFU potential, primary and secondary in vivo repopulation, and the ability to efficiently contribute to the most primitive HSPC WBM compartments (HSC and MPP). These data suggest that *Foxa3*$^{-/-}$ BM contains fewer repopulating cells than *Foxa3*$^{+/+}$ marrow and that self-renewal may be compromised in *Foxa3*$^{-/-}$ HSCs.

FOXA3-binding motifs are enriched in LT-HSC enhancers and target proliferative and stress pathways

To begin to understand how *Foxa3* regulates HSC function, we asked whether the FOXA3 binding motif is significantly enriched in active and/or poised enhancers in long-term HSCs (LT-HSCs) and progeny (Lara-Astiaso et al., 2014). We found the FOXA3-binding motif enriched in enhancers active in LT-HSCs but poised in downstream populations (Table S4), suggesting that *Foxa3* likely functions at the level of the LT-HSCs, which agrees with our finding that *Foxa3* is most highly expressed in HSCs (Fig. 6 A). These enhancers were not enriched for any other known transcription factor binding motifs, suggesting that *Foxa3* either acts alone at these sites or cooperates with regulators whose motifs have not yet been defined (unpublished data). We next used IM-PET (Integrated Method for Predicting Enhancer Targets) to identify the promoters likely targeted by these FOXA3-binding motif$^+$ enhancers (Table S5; He et al., 2014). The resulting gene set was expressed higher than the rest of the genes in our microarray data (*Foxa3*$^{+/+}$ HSC versus *Foxa3*$^{-/-}$ HSC), confirming regulation of these genes by *Foxa3* in LT-HSCs (Fig. 7 A and Table S6). Gene Ontology (GO) enrichment analysis (Ashburner et al., 2000) of this gene set yielded terms including cell cycle (mitotic cell cycle and DNA replication), metabolism (nucleic acid biosynthesis and peptidyl-asparagine modification), and stress (ER overload response, response to ER stress, ER-nuclear signaling pathway) as putative regulated processes (Table S7). Ingenuity Pathway analysis yielded multiple pathways that matched our gene set because of a common signature that included: *Myc*, *Fos*, *Stat5a*, *PIK3CA*, *Nras*, *Grb2*, *PIK3CG*, *SOS1*, and *Stat3* (Table S8). These are molecules commonly found downstream of growth and cytokine receptors that in-

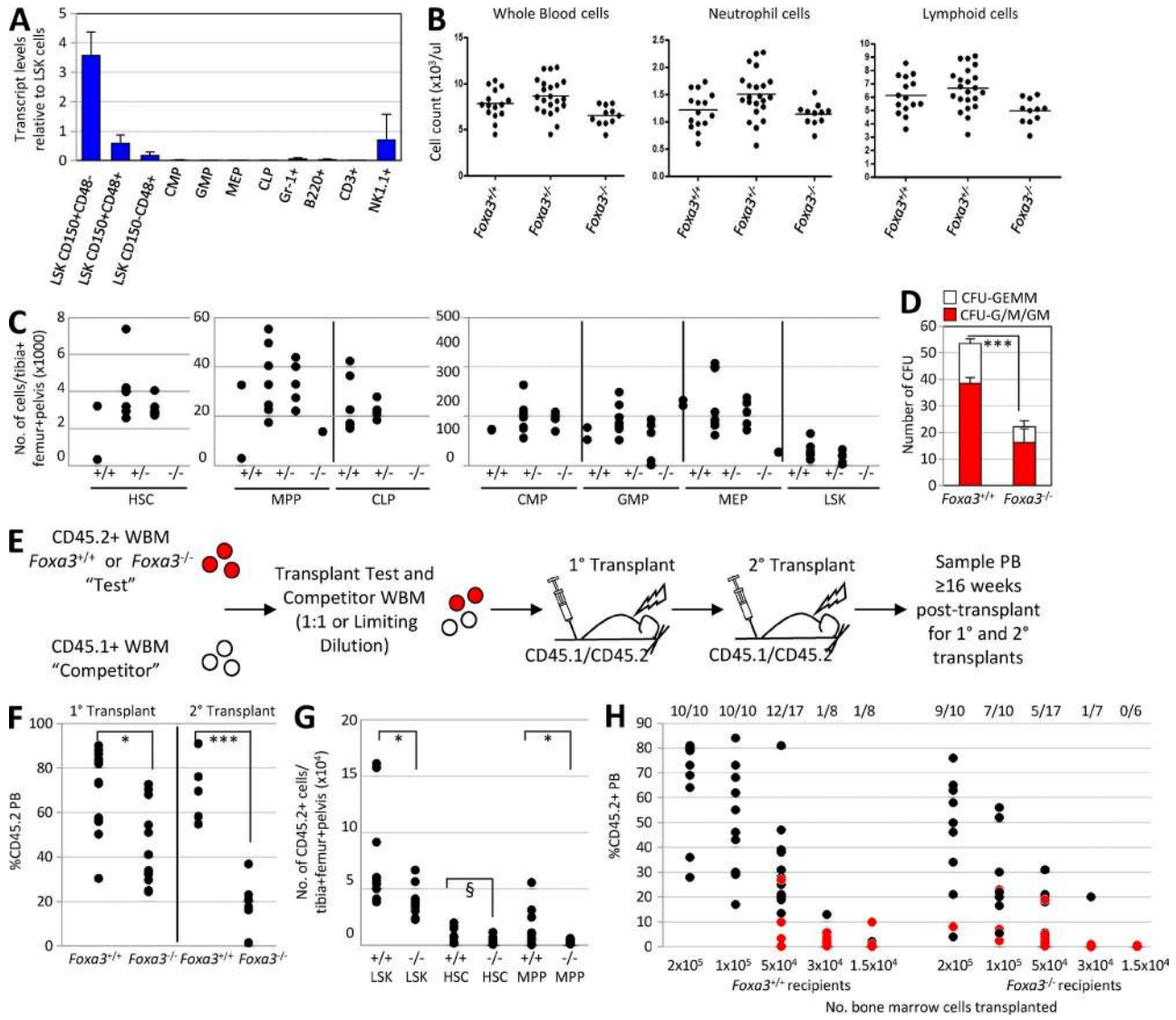

Figure 6. ***Foxa3* is dispensable for native hematopoiesis but required for HSC repopulating potential.** (A) qRT-PCR of *Foxa3* transcript. (B) PB counts of $Foxa3^{+/+}$, $Foxa3^{-/+}$, and $Foxa3^{-/-}$ littermates. (C) Absolute number of HSPCs in one femur + one tibia + one pelvis of 6–10-wk-old $Foxa3^{-/-}$ (n = 5), $Foxa3^{-/+}$ (n = 6), and $Foxa3^{+/+}$ (n = 2) littermates. In B and C, each circle represents an independent mouse. (D) CFU activity of 150 $Foxa3^{-/-}$ (n = 5) or $Foxa3^{+/+}$ (n = 5) HSCs. Error bars = SD. P = 6.2 × 10^{-6}. (E) Schematic showing $Foxa3^{-/-}$ or $Foxa3^{+/+}$ HSC strategies. (F) For first degree transplants, $CD45.2^+$ $Foxa3^{-/-}$ or $Foxa3^{+/+}$ WBM was transplanted with $CD45.1^+$ WBM into ablated $CD45.1^+/CD45.2^+$ recipients in a 1:1 ratio. Percentage of $CD45.2^+$ recipient PB at 20 wk after transplant is shown (*, P = 0.03). For 2° transplants, $CD45.2^+$ WBM was isolated from 1° recipients 16 wk after transplant and transplanted into ablated $CD45.1^+/CD45.2^+$ mice. %$CD45.2^+$ recipient PB is shown 16 wk after transplant for 2° transplant recipients (***, P = 0.0001). Each circle is an independently transplanted mouse. (G) The LSK, HSC, and MPP compartments of 1° recipients of $CD45.2^+$ $Foxa3^{-/-}$ (n = 12) or $Foxa3^{+/+}$ (n = 11) cells were examined >16 wk after transplant for the absolute number of $CD45.2^+$ cells (shown as number of cells/one femur + one tibia + one pelvis). Each circle is an independent mouse. P = 0.02, 0.08, and 0.04, respectively. (H) 15,000, 30,000, 50,000, 100,000, or 200,000 $CD45.2^+$ $Foxa3^{-/-}$ or $Foxa3^{+/+}$ WBM cells were transplanted with $CD45.1^+$ WBM into $CD45.1^+/CD45.2^+$ recipients. Recipients were scored as repopulated if their $CD45.2^+$ PB chimerism was >1% in the T cell, B cell, and myeloid cell lineages 10–16 wk after transplant (data are the pooled results of two independently performed limiting dilution transplants). Each circle is an individual recipient (black circles label engrafted mice and red circles label nonengrafted mice). The number of mice engrafted/number of mice transplanted at each cell dose is shown. Significantly fewer repopulating HSCs were detected in $Foxa3^{-/-}$ WBM than $Foxa3^{+/+}$ WBM (P = 0.0046). χ^2 analysis revealed a fit to the limiting dilution model (Table S3). These analyses were performed using L-Calc.

terface with survival, cell cycle, and metabolic signaling. Unfolded Protein Response and Endoplasmic Reticulum Stress Pathways also matched to our dataset. Top Predicted Regulators included *Myc*, *TP53*, and *TGFβ* (Table S8). Finally, GSEA analysis also returned categories indicative of perturbed stress, signaling, and metabolic pathways (e.g., apoptosis by doxyru-

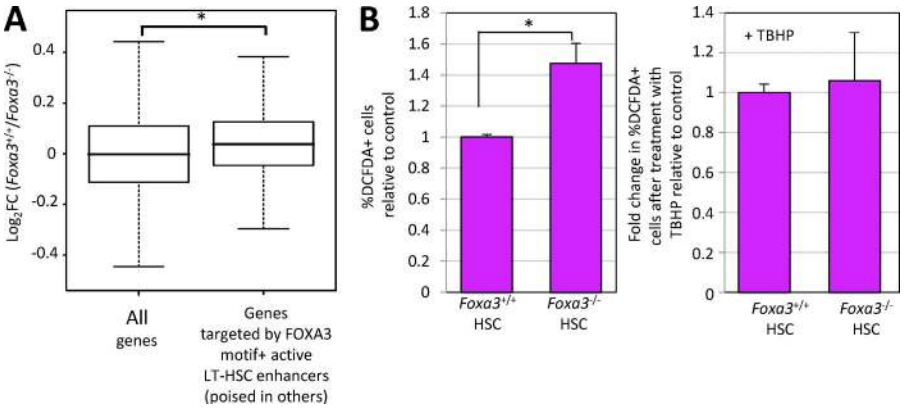

Figure 7. ***Foxa3* protects HSCs from cellular stress.** (A) Genes predicted by IM-PET to be targets of FOXA3 binding motif$^+$ LT-HSC enhancers (Table S5) are significantly more perturbed in expression among genes differentially expressed between *Foxa3*$^{-/-}$ and *Foxa3*$^{+/+}$ HSCs (Table S6). P = 2.6×10^{-29}. (B) CD45.2$^+$ LSK CD150$^+$CD48$^-$ cells were isolated from first degree recipients of *Foxa3*$^{+/+}$ ($n = 6$) and *Foxa3*$^{-/-}$ ($n = 7$) BM and then stained with DCFDA to assess endogenous ROS levels (left) or treated with TBHP before DCFDA staining to induce elevated ROS (right). Values represent the percentage of cells positive for DCF DA in *Foxa3*$^{-/-}$ cells relative to *Foxa3*$^{+/+}$ cells (left) or the relative fold change of DCFDA$^+$ cells in *Foxa3*$^{-/-}$ versus *Foxa3*$^{+/+}$ CD45.2$^+$ LSK CD150$^+$CD48$^-$ after TBHP treatment (right). For the left graph, P = 0.001 (*). P-values were calculated via exact Wilcoxon Mann-Whitney test.

bicin, up in CML, biopolymer metabolic process; Table S9). Cumulatively, these analyses implicate *Foxa3* in the regulation of HSC metabolic and proliferative stress. To explore this further, CD45.2$^+$ HSCs (i.e., LSK CD150$^+$CD48$^-$ cells) were isolated from recipients of CD45.2$^+$ *Foxa3*$^{+/+}$ or *Foxa3*$^{-/-}$ WBM >8 mo after transplant and examined by staining with 2′,7′-dichlorofluorescin diacetate (DCFDA) for reactive oxygen species (ROS). *Foxa3*$^{-/-}$ HSCs displayed a 50% increase in ROS relative to Foxa3$^{+/+}$ HSCs (P = 0.006; Fig. 7 B). Despite the increase in basal ROS levels, *Foxa3*$^{-/-}$ HSCs were able to recover from induced ROS similar to control HSCs (Fig. 7 B). These data confirm bioinformatics predictions that *Foxa3*$^{-/-}$ HSCs are subject to elevated metabolic stress. Further work will be required to determine exactly how *Foxa3* contributes to the control of ROS levels in HSCs.

In sum, *Foxa3* is dispensable to the hematopoietic compartment during homeostasis (Fig. 6, B and C), yet critical for optimal HSC function after transplant (Fig. 6 F). Under these conditions, activation of pathways regulating proliferation and metabolism is key. Indeed, the *Foxa3*$^{-/-}$ repopulating phenotype is most dramatic when greater pressure to repopulate is placed on individual cells (e.g., in limiting dilution transplants and serial transplantation; Fig. 6 H) and *Foxa3*$^{-/-}$ HSCs display a significant increase in ROS, which is known to compromise HSC self-renewal, maintenance, and repopulating potential (Ito et al., 2006; Jang and Sharkis, 2007; Tothova et al., 2007; Taniguchi Ishikawa et al., 2012).

DISCUSSION

Here, we report a transplant-based screen for novel regulators of HSPC engraftment. By minimizing the ex vivo culture of HSPCs before transplant (24–44 h), we focused our study on identifying regulators of HSPC repopulation. Our approach used multiple independent shRNAs targeting prioritized gene candidates. Each shRNA was functionally validated to mediate robust gene knockdown in primary LSK cells (Fig. 1 D). To ensure high resolution of hits from non-hits, we verified robust cell transduction for each experiment in our functional screen (Fig. 2 B). Further, each putative hit was validated by retesting, thereby minimizing the likelihood of false positives caused by off-target effects or viral integration. More than 1,300 mice were transplanted to complete this study. These variables combined to yield a hit rate of 41.5% (17/41 genes tested), illustrating the robustness of our approach and the fidelity of the publically available bioinformatics resources from which our gene candidates were drawn (Chambers et al., 2007; Heng and Painter, 2008; McKinney-Freeman et al., 2012).

We identified 17 new functional regulators of LSK cell in vivo repopulating activity: 15 are required for optimal repopulation (*Arhgef5*, *Cadps2*, *Crispld1*, *Emcn*, *Foxa3*, *Fstl1*, *Glis2*, *Gpr56*, *Myct1*, *Nbea*, *P2ry14*, *Smarca2*, *Sox4*, *Stat4*, and *Zfp521*) and 2 are negative regulators (*Armcx1* and *Gprasp2*). 12 of these genes have never been implicated in HSPC biology, although 5 (e.g., *P2ry14*, *Smarca2*, *Sox4*, and *Gpr56*) have recently been shown to play an important role in leukemia or HSCs (Zhang et al., 2013; Buscarlet et al., 2014; Cho et al., 2014; Solaimani Kartalaei et al., 2015). These studies confirm that our screen has identified genes relevant to HSC function. Prior screens of mouse and human HSPCs involved extensive culture (12–17 d) before transplant or followed the preservation of a stem cell phenotype or colony formation during culture (5 d to 10 wk; Ali et al., 2009; Deneault et al., 2009; Boitano et al., 2010; Hope et al., 2010), thus biasing their read-out for genes involved in self-renewal or stem cell maintenance, two processes critical to HSC function and culture. By minimizing LSK cell culture before transplant, we reasoned that our screen would identify genes regulating not only self-renewal, which can enhance HSPC repopulation, but also distinct cellular processes critical to the long-term reconstitution of an ablated hematopoietic system that may

not have been as readily discernable in these prior studies (e.g., niche lodgement and retention, survival under stress, activation, and differentiation).

Prior studies also often focused on specific molecular processes (e.g. nuclear factors, polarity and asymmetric division, and histone methylation). Our screen was unbiased in that our two criteria were (1) confirmation by qRT-PCR of high expression in LSK cells and (2) identification of effective shRNAs. This approach discovered hits involved in distinct cellular and molecular processes, some currently understudied in HSPCs. For example, multiple likely regulators of vesicular trafficking and cell surface receptor turnover were identified as regulators of LSK cell repopulating activity (*Nbea*, *Cadsps2*, *Armcx1*, and *Gprasp2*; Cisternas et al., 2003; Abu-Helo and Simonin, 2010; Moser et al., 2010; Niesmann et al., 2011; Fig. 3). These genes may regulate stable HSPC–niche interactions or the transduction of key survival signals during hematopoietic stress. Indeed, changes in CFU activity, cell cycle, and apoptosis in LSK cells maintained ex vivo after knockdown of *Nbea*, *Cadps2*, or *Gprasp2* (Fig. 5), suggest regulation of intrinsic pathways controlling differentiation, survival, and/or proliferation by these genes.

Arhgef5, a Rho guanine nucleotide exchange factor, has been implicated in podosome formation (Kuroiwa et al., 2011). Podosomes are important for cell adhesion and migration. Knockdown of *Arhgef5* in LSK cells maintained ex vivo resulted in an accumulation of cells in G_1, as well as a loss of total CFU formation (Fig. 5 A and B). *Gpr56*, previously implicated in neuronal migration, was recently shown to participate in HSC development and adhesion. *Gpr56*$^{-/-}$ HSCs also display a repopulating defect, as seen in our study after gene knockdown (Saito et al., 2013; Singer et al., 2013; Rao et al., 2015; Solaimani Kartalaei et al., 2015). We also identified secreted molecules (*Fstl1* and *Crispld1*). *Fstl1* is a TGFβ and BMP antagonist, whereas *Crispld1* is likely a protease that targets the extracellular matrix (Gibbs et al., 2008; Geng et al., 2011). Knockdown of *Fstl1* in LSK cells led to fewer CFUs and loss of the LSK cell surface phenotype, suggesting an intrinsic loss of HSPC potential (Fig. 5). These genes suggest that, to facilitate stable engraftment and in vivo repopulation, HSPCs may autonomously condition their niche and culture by countering inhibitory signaling pathways (e.g., TGFβ) and remodeling the extracellular matrix (*Arhgef5* and *Crispld1*).

Although *Myct1* has never been implicated in HSPC function, it is a c-*Myc* target that modulates HSC–niche interactions via N-cadherin (Wilson et al., 2004). There are currently no primary articles on *Zfp521*, a Krueppel-type C2H2 zinc finger gene family member and possible transcriptional repressor, given it contains a KRAB domain (Urrutia, 2003). Knockdown of this gene in LSK cells perturbed CFU formation, appeared to enhance survival ex vivo, and led to a dramatic loss of chimerism downstream of the HSC compartment in the BM of transplanted mice, suggesting that *Zfp521* regulates the differentiation and survival of HSPCs (Fig. 5). Although several of our hits are known to be expressed by HSPCs or have been implicated in leukemogenesis, here we show them to be regulators of HSPC repopulation (*Emcn*, *Glis2*, *Sox4*, and *Smarca2*; Matsubara et al., 2005; Gruber et al., 2012; Masetti et al., 2013; Zhang et al., 2013; Buscarlet et al., 2014; Ma et al., 2014). Finally, our hit, the purinergic receptor *P2ry14*, was very recently shown to be an essential regulator of stress hematopoiesis and HSC repopulation, further validating our screen (Cho et al., 2014). Globally, the results of our screen support a model in which active cross talk between the BM niche and HSPCs is essential for stable hematopoietic repopulation after transplant. Thus, exogenous treatment of HSCs with *Fstl1* and *Crispld1* may promote their stable engraftment. Indeed, it was recently reported that *Fstl1*, which is also expressed in cardiac epicardium, promotes the regeneration of cardiomyocytes both in vivo and ex vivo (Wei et al., 2015). This remains to be tested in HSPCs. Each hit identified here is a window into the processes that regulate the in vivo repopulating activity of HSPCs and warrant further investigation.

Although homing is critical to HSPC engraftment, our screen was not technically designed to identify homing regulators: in our system, maximum gene knockdown occurs 48–72 h after transduction (Holmfeldt et al., 2013). Transduced Test cells are transplanted 24–44 h after transduction, before full gene knockdown. Thus, further work is required to determine whether any of the hits identified here regulate HSC homing.

We identified *Foxa3* as a novel regulator of HSPC repopulation (Fig. 2 C and Fig. 3 E). *Foxa* genes have never before been implicated in HSPC biology. We found that *Foxa3* is highly expressed by HSCs (Fig. 6 A) and, although *Foxa3*$^{-/-}$ mice display normal hematopoiesis (Fig. 6, B and C), *Foxa3*$^{-/-}$ HSCs are deficient in CFUs and primary and secondary in vivo repopulation (Fig. 6, D–F). Other genes are also known to be dispensable for homeostasis but are absolutely required for HSC function under pathophysiological conditions, such as hematopoietic stress (e.g., *p21*, β-*catenin*, *FoxOs*, *Gadd45a*, and *Gab2*; Cheng et al., 2000; Zhang et al., 2007; Zhao et al., 2007; Chen et al., 2014). Indeed, *P2ry14*, also identified here, is not required for steady-state hematopoiesis but is essential for HSC function after stress and injury (Cho et al., 2014). Thus, mechanisms that preserve the hematopoietic compartment during stress (e.g., after transplantation) are often not required for homeostasis, and *Foxa3* appears to be a newly discovered regulator of these processes. Indeed, genes targeted by active LT-HSC enhancers containing FOXA3-binding motifs were enriched for pathways controlling cell cycle, metabolism, and stress, and *Foxa3*$^{-/-}$ HSCs display a significant increase in ROS content (Fig. 7 B and Tables S4 and S7–S9). Increased ROS levels are known to compromise HSC self-renewal, quiescence, and repopulating potential (Ito et al., 2006; Jang and Sharkis, 2007; Tothova et al., 2007; Taniguchi Ishikawa et al., 2012). *Foxa3*$^{-/-}$ HSC's failure to efficiently repopulate ablated mice was most pronounced when limiting cell numbers were transplanted and after serial transplantation (Fig. 6 H). These are both scenarios in which the pressure on

individual repopulating cells to expand and differentiate is extreme. In contrast, during homeostasis, when the pressure on individual cells to maintain steady-state hematopoiesis is low, *Foxa3* is dispensable. Thus, in the absence of *Foxa3*, HSPCs fail to respond efficiently to hematologic stress.

HSPC in vivo repopulating activity is complex, requiring the orchestration of many molecular and cellular processes. This is evident by the disparate putative functions of the molecules identified in our screen. There is a burgeoning interest in better understanding the regulation of stable HSPC engraftment, as manipulating this process represents a promising strategy for improving the efficiency of HSCT. Our study represents a valuable resource that will catalyze investigation into novel cellular mechanisms that may control this process. The better we understand the full scope of the cellular mechanisms that regulate stable HSPC engraftment, the better equipped we will be to develop novel therapies to improve HSCT outcomes.

MATERIALS AND METHODS

Mice. C57BL/6J and C57BL/6.SJL-PtprcaPep3b/BoyJ mice were acquired from The Jackson Laboratory and housed in a pathogen-free facility. All animal experiments were performed according to procedures approved by the St. Jude Children's Research Hospital Institutional Animal Care and Use Committee. C57BL/6 *Foxa3*$^{-/-}$ mice were a gift from the laboratory of K. Kaestner (University of Pennsylvania, Philadelphia, PA).

Genotyping. PCRs were performed using GoTaq DNA Polymerase (Promega) and performed as indicated by the manufacturer. PCR conditions: 95°C, 2 min; (95°C, 30 min; 60°C, 30 min; 72°C, 30 min) × 35; 72°C, 10 min. Primers: *Foxa3* F2 (5′-ACATGACCTTGAACCCACTC-3′), *Foxa3* R1 (5′-TAGTACGGGAAGAGGTCCAT-3′), *Foxa3* LacZ3 (5′-AATGTGAGCGAGTAACAACC-3′). WT PCR, *Foxa3* F2^{+} *Foxa3* R1; WT band, 349 bp. KO PCR, *Foxa3* F2^{+} *Foxa2* LacZ3; Knock-out band, 648 bp. qRT-PCR total RNA isolated from 70,000 LSK cells (RNeasy Micro kit; QIAGEN) was reversed transcribed into cDNA (High Capacity cDNA Reverse Transcriptional kit with RNase Inhibitor; Invitrogen). qRT-PCR was performed using Fast SYBR Green Master Mix (Applied Biosystems) on an ABI StepOnePlus thermal cycler (Applied Biosystems) according to the manufacturer's instructions. PCR program: 95°C for 20 min; (95°C for 1 min and 60°C for 20 min) × 40; (Melt curve) 95°C for 15 min; 60°C for 15 min; and 95°C for 15 min. *Tbp* expression levels were used to compensate for differences in cDNA input. ΔΔCt method was applied to calculate changes in gene expression. Primers were used at 0.4 μM. Primer sequences are listed in Table S1.

shRNAs. shRNAs were designed as previously described (Table S2; Fellmann et al., 2011; Holmfeldt et al., 2013). Gene knockdown efficiency in LSK cells was quantified by qRT-PCR and normalized to transduction frequency (Table S2).

Lentiviral production. Vesicular stomatitis virus glycoprotein–pseudotyped lentivirus was prepared as previously described via a four plasmid system (Transfer vector-, Gag/Pol-, Rev/Tat-, and vesicular stomatitis virus glycoprotein envelope plasmid) by co-transfection of 293T cells using T*ransIT 293* (Mirus; Holmfeldt et al., 2013). Viral supernatant was collected 48 h later, cleared, and stored at −80°C. Viral preparations were titered on 293T cells.

LSK cell culture and transduction. LSK cells were isolated from 6–10-wk-old murine BM and transduced with lentivirus as previously described (Holmfeldt et al., 2013). In brief, nontissue culture 96-well plates were coated with Retronectin (TaKaRA Bio) according to the manufacturer's instructions. Lentiviral particles corresponding to a multiplicity of infection (MOI) of 25 were spin loaded onto the plates for 1 h at 1,000 *g* at room temperature. Wells were washed with PBS, followed by the addition of 15,000 freshly isolated LSK cells resuspended in 200 μl serum-free expansion medium (STEMCELL Technologies) with 10 ng/ml recombinant murine (RM) stem cell factor (SCF), 20 ng/ml RM thrombopoietin (Tpo), 20 ng/ml RM insulin-like growth factor 2 (IGF-2; PeproTech), 10 ng/ml recombinant human (RH) fibroblast growth factor 1 (FGF-1; R&D Systems), and 5 μg/ml protamine sulfate (Sigma-Aldrich). Cells were incubated overnight at 37°C. To collect cells for transplantation the next morning, media was slowly removed and cells were washed and resuspended in PBS + 1.5% FCS.

To compare the transduction efficiency of LSK cells versus LSK CD150^{+}CD48^{-} cells, these cells were isolated in parallel as previously described (Holmfeldt et al., 2013). 2,500 cells were transduced on graded concentrations of indicated viruses in retronectin-coated 96-well plates as described above. Transduction frequencies were analyzed 4 d after transduction using flow cytometry. To assess any nonspecific effect of shRNAs on the viability of primitive hematopoietic cells, LSK cells transduced with lentivirus were cultured for 2 wk in serum-free expansion medium (STEMCELL Technologies) with 10 ng/ml RM-SCF, 20 ng/ml RM thrombopoietin (Tpo), 20 ng/ml RM IGF-2 (PeproTech), 10 ng/ml RH-FGF-1 (R&D Systems), and 10 μg/ml heparin (Sigma-Aldrich). The persistence of mCherry^{+} cells was monitored using an LSR Fortessa (BD) and FlowJo version 9.4.11 (Tree Star).

BM transplants. Recipients were treated with 11 Gy of ionizing radiation in split doses of 5.5 Gy. For the functional screen, 5,000 CD45.2^{+} Test LSK cells were injected 24 h after transduction with 5,000 mock-transduced CD45.1^{+} Competitor LSK cells into recipients by tail vein. For retesting of hits, 5,000 CD45.2^{+} Test mCherry^{+}/LSK cells were isolated by FACS 44 h after transduction and injected with 5,000 mock-transduced and mock-sorted CD45.1^{+} Competitor LSK cells by tail vein. For 1:4 Test versus Competitor transplants, 2,000 CD45.2^{+} Test mCherry^{+}/LSK cells were isolated by FACS 44 h after transduction and trans-

planted with 8,000 mock-transduced and mock-sorted CD45.1$^+$ competitor LSK cells.

For investigating *Foxa3*, 4 × 10^5 CD45.2$^+$ *Foxa3*$^{+/+}$ or *Foxa3*$^{-/-}$ WBM cells were injected with 4 × 10^5 CD45.1$^+$ WBM cells into lethally irradiated CD45.1$^+$/CD45.2$^+$ recipients by tail vein. For secondary transplants, 4 × 10^5 CD45.2$^+$ WBM cells sorted from primary recipients of *Foxa3*$^{+/+}$ or *Foxa3*$^{-/-}$ WBM cells were transplanted with 4 × 10^5 CD45.1$^+$ WBM WT competitor cells into lethally irradiated CD45.1$^+$/CD45.2$^+$ recipients. For limiting dilution transplants, 15,000, 30,000, 50,000, 100,000, or 200,000 CD45.2$^+$ *Foxa3*$^{+/+}$ or *Foxa3*$^{-/-}$ WBM cells were injected with 2 × 10^5 CD45.1$^+$ WBM cells into lethally irradiated CD45.1$^+$/CD45.2$^+$ recipients by tail vein in two independent experiments. Engraftment was defined as >1% CD45.2 chimerism in the T cell, B cell, and myeloid lineages of recipient PB 10–16 wk after transplant. L-Calc (STEMCELL Technologies) was used to analyze the results of the limiting dilution transplants.

Antibodies for WBM and PB analysis. All antibodies used in this study for the analysis of WBM and PB cell populations by flow cytometry are as previously described (Holmfeldt et al., 2013).

Analysis of PB. PB was collected from the retro-orbital plexus in heparinized capillary tubes and lysed in red blood cell lysis buffer (Sigma-Aldrich). Cells were stained with the following antibodies: CD45.1-FITC, CD45.2-APC, (B220, Gr1, Cd11b)-PerCPCy5.5, and (B220, CD4, CD8)-PECy7 (BD), followed by flow cytometry analysis using an LSR Fortessa and data analysis using FlowJo version 9.4.11.

CFU assays. For analysis of CFU potential of LSK cells after knockdown of screen hits, LSK cells were transduced overnight with control or gene-specific shRNAs, and then cultured at 15,000 cells/well in non-tissue culture–treated 96-well plates for 5–6 d in serum-free expansion medium (STEMCELL Technologies) with 10 ng/ml RM SCF, 20 ng/ml RM Tpo, 20 ng/ml RM IGF-2 (PeproTech), 10 ng/ml RH FGF-1 (R&D Systems), and 10 µg/ml heparin (Sigma-Aldrich). 500 mCherry$^+$ LSK cells were then isolated by FACS and plated in M3434 methylcellulose (STEMCELL Technologies). For CFU analysis of *Foxa3*$^{+/+}$ or *Foxa3*$^{-/-}$ HSCs, 150 HSCs (LSK CD150$^+$CD48$^-$) were isolated by FACS from WBM, and then plated in M3434. Colonies were analyzed 10 d after plating.

Cell cycle analysis of shRNA-transduced LSK cells. LSK cells were transduced overnight with control or gene-specific shRNAs and then cultured at 15,000 cells/well in nontissue culture treated 96-well plates for 5–6 d in serum-free expansion medium (STEMCELL Technologies) with 10 ng/ml RM SCF, 20 ng/ml RM Tpo, 20 ng/ml RM IGF-2 (PeproTech), 10 ng/ml RH FGF-1 (R&D Systems), and 10 µg/ml heparin (Sigma-Aldrich). mCherry$^+$ LSK cells were then collected by FACS and stained with the following antibodies: (B220, CD3, CD4, CD8, CD19, Gr-1, and Ter119)-PerCP, Sca-1-PerCP-Cy5.5, and c-Kit-APC-780. Cells were then fixed using the Cytofix/Cytoperm kit (BD), followed by staining for Ki67-FITC (Clone SolA15; eBioscience) and DAPI. Cells were analyzed via an LSR Fortessa and FlowJo version 9.4.11.

Apoptosis analysis of shRNA-transduced LSK cells. LSK cells were transduced overnight with control or gene-specific shRNAs and then cultured at 15,000 cells/well in non-tissue culture–treated 96-well plates for 5–6 d in serum-free expansion medium (STEMCELL Technologies) with 10 ng/ml RM SCF, 20 ng/ml RM Tpo, 20 ng/ml RM IGF-2 (PeproTech), 10 ng/ml RH FGF-1 (R&D Systems), and 10 µg/ml heparin (Sigma-Aldrich). Cells were collected 5–6 d after plating and stained with the following antibodies: (B220, CD3, CD4, CD8, CD19, Gr-1, and Ter119)-PerCP, Sca-1-PerCP-Cy5.5, and c-Kit-APC-780. After staining for surface antigens, cells were labeled with Annexin V-FITC (BD) and DAPI, and then analyzed using an LSR Fortessa and FlowJo version 9.4.11.

Analysis of total blood counts in Foxa3 mice. PB was harvested from the retro-orbital plexus in heparinized capillary tubes and analyzed on a Forcyte instrument (Oxford Scientific).

Analysis of HSPCs in transplant recipients and Foxa3 mice. Tibias, femurs, and pelvic bones were removed from mice and BM isolated by crushing. BM was then lysed in red blood cell lysis buffer (Sigma-Aldrich). Donor-derived HSCs (LSK CD150$^+$CD48$^-$), MPPs (LSK Flt3L$^+$), common myeloid progenitors (CMPs; Lineage$^-$c-Kit$^+$Sca-1$^-$FcR^{low}CD34$^+$), common lymphoid progenitors (CLPs; Lineage$^-$c-Kit^{Low} Sca-1^{Low}IL7R$^+$), granulocyte-myeloid progenitors (GMPs; Lineage$^-$c-Kit$^+$Sca-1$^-$FcR^{high}CD34$^+$), and megakaryocyte-erythroid progenitors (MEPs; Lineage$^-$c-Kit$^+$Sca-1$^-$FcR$^-$CD34$^-$) were visualized in transplant recipients by staining with the following antibodies: HSC ([B220, CD3, CD4, CD8, CD19, Gr-1, Ter119]-PerCP, Sca-1-PerCP-Cy5.5, c-Kit-APC-780, CD150-PE-Cy7, CD48-Alexa Fluor 700, CD45.1-FITC, and CD45.2-v500); CMP/GMP/MEP ([B220, CD3, CD4, CD8, CD19, Gr-1, Ter119]-PerCP, Sca-1-PerCP-Cy5.5, c-Kit-APC-780, FcR II/III-Alexa Fluor 700, CD34-FITC, CD45.1-APC, and CD45.2-v500); and CLP/MPP (B220, CD3, CD4, CD8, CD19, Gr-1, Ter119)-PerCP, Sca-1-PerCP-Cy5.5, c-Kit-APC-780, IL-7R-PE-Cy7, Flt3-APC, CD45.1-FITC, and CD45.2-v500. HSPCs were visualized in *Foxa3*$^{-/-}$ and *Foxa3*$^{+/+}$ mice as described above with the exclusion of CD45.1 and CD45.2. Cells were then analyzed using an LSR Fortessa and data analysis was done using FlowJo version 9.4.11. DAPI (Sigma-Aldrich) was used for dead cell exclusion.

Analysis of FOXA3-binding motifs in HSC enhancers and gene targets. Active and poised enhancers in LT-HSC, ST-HSC, MPP, and GMP were obtained from the enhancer compendium generated by Lara-Astiaso et al. (2014). These enhancers were identified based on their histone modification signatures. For FOXA3

motif analysis, we downloaded the position weight matrix of FOXA3 motif from the Cis-BP database (Weirauch et al., 2014). We used FIMO to scan the enhancer sequences for the occurrence of FOXA3 binding motifs with a p-value threshold of 10^{-5} (Grant et al., 2011). To predict the target genes of FOXA3 binding motif^{+} enhancers, we used the integrated method for predicting enhancer targets (IM-PET) software (He et al., 2014), which predicts enhancer-promoter interactions by integrating transcriptomic, epigenomic, and genomic sequence information. Histone modification and RNA-Seq data acquired by IM-PET were from (Cabezas-Wallscheid et al., 2014; Lara-Astiaso et al., 2014). The predicted targets of FOXA3-binding motif^{+} enhancers in LT-HSCs were extracted for GSEA analysis.

Foxa3 microarray. Total RNA was isolated from 10,000 *Foxa3*$^{+/+}$ or *Foxa3*$^{-/-}$ HSCs using the RNeasy Micro kit (QIAGEN). RNA was amplified by the NuGEN Ovation Pico WTA V2 system and labeled using the NuGEN Encore Biotin Module (NuGen). Labeled targets were hybridized on the HT MG-430 PM plate array and processed using the GeneTitan system (Affymetrix). Array data were quantile normalized and robust multi-array average summarized in Genomics Suite 6.6 (Partek). The complete dataset is deposited in the Gene Expression Omnibus (GSE63830.).

Analysis of ROS content in Foxa3$^{+/+}$ and Foxa3$^{-/-}$ HSCs. *Foxa3*$^{+/+}$ and *Foxa3*$^{-/-}$ WBM was isolated, magnetically enriched for c-Kit^{+} cells, and then stained with Sca-1-PerCP-Cy5.5, c-Kit-APC-780, CD150-PE-Cy7, and CD48-Alexa Fluor 700. Cells were then treated with vehicle or 500 µM tert-butyl Hydrogen Peroxide (TBHP). 3 h after treatment, cells were stained with 5 µM DCFDA for 30 min on ice and then analyzed via an LSR Fortessa and FlowJo version 9.4.11. The peak excitation wavelength for oxidized DCF was 488 nm and emission was 525 nm.

Statistics. Statistical significance for comparisons between two groups was assessed using two sample *t* tests or exact Wilcoxon Mann-Whitney tests, depending on the normality test based on the Shapiro-Wilk test. Measurements for each gene were normalized to their respective control and a one sample *t* test was performed to assess if the mean of the normalized measurements is equal to one. All these analyses were performed in SAS version 9.3. For limiting dilution analysis (LDA), parameters were estimated using a generalized linear model with a complementary log-log link. χ^2 (Pearson and Deviance) were used to assess the goodness-of-fit to the LDA model. Differences in the frequency of HSCs between *Foxa3*$^{+/+}$ and *Foxa3*$^{-/-}$ mice were assessed by relying on the asymptotic normality of the maximum likelihood estimation. LDA were performed using L-Calc (STEMCELL Technologies). All the reported p-values are two-sided and considered statistically significant if $P < 0.05$, although $P < 0.1$ is also noted in some instances as marginally significant.

Online supplemental material. Fig. S1 presents gating flow cytometry gating strategies for the ex vivo analysis of cell cycle, cell surface phenotype, and apoptosis. Table S1 presents qRT-PCR primer sequences. Table S2 presents a summary of genes tested in functional screen and corresponding shRNA sequences. Table S3 presents *Foxa3*$^{-/-}$ and *Foxa3*$^{+/+}$ WBM predicted repopulating cell frequency, along with their 95% confidence interval based on limiting dilution transplant. Table S4 presents FOXA3 binding motif enrichment in enhancers active in LT-HSCs and poised in other HSPC compartments (Lara-Astiaso et al., 2014). Table S5 presents predicted gene targets of *Foxa3* motif^{+} active LT-HSC enhancers. Table S6 presents microarray results of *Foxa3*$^{-/-}$ HSCs versus *Foxa3*$^{+/+}$ HSCs. Table S7 presents GO analysis results. Table S8 presents Ingenuity pathway analysis. Table S9 presents GSEA analysis results. Online supplemental material is available at http://www.jem.org/cgi/content/full/jem.20150806/DC1.

ACKNOWLEDGMENTS

We thank Sandy Schwemberger and Richard Ashmun of St. Jude Children's Research Hospital Flow Cytometry Core for FACS support, Cara Davis-Goodrum and Chandra Savage in the St. Jude Children's Research Hospital Animal Research Core for their help with injections, and Klaus Kaestner (University of Pennsylvania, Philadelphia, PA) for *Foxa3*$^{-/-}$ mice. We thank Kevin Freeman, Teresa Bowman, and the McKinney-Freeman laboratory for manuscript commentary. We also thank Lucas Van Tol and the University of Iowa Institute for Clinical and Translational Science for computing support.

This work was supported by grants from the American Society of Hematology (S. McKinney-Freeman), the National Institute of Diabetes and Digestive and Kidney Diseases (K01DK080846; S. McKinney-Freeman), the National Human Genome Research Institute (HG006130; K. Tan), and funding from the American Lebanese Syrian Associated Charities (S. McKinney-Freeman).

P. Holmfeldt received a stem cell grant from BD. The authors declare no additional competing financial interests.

Author contributions: P. Holmfeldt, M. Ganuza, H. Marathe, K. Tan, and S. McKinney-Freeman designed the research; P. Holmfeldt, M. Ganuza, H. Marathe, B. He, T. Hall, J. Pardieck, A.C. Saulsberry, A. Cico, L. Gaut, D. McGoldrick, and D. Finkelstein performed the research and collected and analyzed data; G. Kang and J. Moen performed statistical analysis of the data; M. Ganuza, H. Marathe, and S. McKinney-Freeman wrote the paper; and K. Tan and S. McKinney-Freeman supervised the research.

Submitted: 12 May 2015
Accepted: 7 January 2016

REFERENCES

Abu-Helo, A., and F. Simonin. 2010. Identification and biological significance of G protein-coupled receptor associated sorting proteins (GASPs). *Pharmacol. Ther.* 126:244–250. http://dx.doi.org/10.1016/j.pharmthera.2010.03.004

Ali, N., C. Karlsson, M. Aspling, G. Hu, N. Hacohen, D.T. Scadden, and J. Larsson. 2009. Forward RNAi screens in primary human hematopoietic stem/progenitor cells. *Blood.* 113:3690–3695. http://dx.doi.org/10.1182/blood-2008-10-176396

Ashburner, M., C.A. Ball, J.A. Blake, D. Botstein, H. Butler, J.M. Cherry, A.P. Davis, K. Dolinski, S.S. Dwight, J.T. Eppig, et al. The Gene Ontology Consortium. 2000. Gene ontology: tool for the unification of biology. *Nat. Genet.* 25:25–29. http://dx.doi.org/10.1038/75556

Behr, R., S.D. Sackett, I.M. Bochkis, P.P. Le, and K.H. Kaestner. 2007. Impaired male fertility and atrophy of seminiferous tubules caused by haploinsufficiency for Foxa3. *Dev. Biol.* 306:636–645. http://dx.doi.org/10.1016/j.ydbio.2007.03.525

Boitano, A.E., J. Wang, R. Romeo, L.C. Bouchez, A.E. Parker, S.E. Sutton, J.R. Walker, C.A. Flaveny, G.H. Perdew, M.S. Denison, et al. 2010. Aryl hydrocarbon receptor antagonists promote the expansion of human hematopoietic stem cells. *Science.* 329:1345–1348. http://dx.doi.org/10.1126/science.1191536

Buscarlet, M., V. Krasteva, L. Ho, C. Simon, J. Hébert, B. Wilhelm, G.R. Crabtree, G. Sauvageau, P. Thibault, and J.A. Lessard. 2014. Essential role of BRG, the ATPase subunit of BAF chromatin remodeling complexes, in leukemia maintenance. *Blood.* 123:1720–1728. http://dx.doi.org/10.1182/blood-2013-02-483495

Busch, K., K. Klapproth, M. Barile, M. Flossdorf, T. Holland-Letz, S.M. Schlenner, M. Reth, T. Höfer, and H.R. Rodewald. 2015. Fundamental properties of unperturbed haematopoiesis from stem cells in vivo. *Nature.* 518:542–546. http://dx.doi.org/10.1038/nature14242

Cabezas-Wallscheid, N., D. Klimmeck, J. Hansson, D.B. Lipka, A. Reyes, Q. Wang, D. Weichenhan, A. Lier, L. von Paleske, S. Renders, et al. 2014. Identification of regulatory networks in HSCs and their immediate progeny via integrated proteome, transcriptome, and DNA methylome analysis. *Cell Stem Cell.* 15:507–522. http://dx.doi.org/10.1016/j.stem.2014.07.005

Cai, X., L. Gao, L. Teng, J. Ge, Z.M. Oo, A.R. Kumar, D.G. Gilliland, P.J. Mason, K. Tan, and N.A. Speck. 2015. Runx1 deficiency decreases ribosome biogenesis and confers stress resistance to hematopoietic stem and progenitor cells. *Cell Stem Cell.* 17:165–177. http://dx.doi.org/10.1016/j.stem.2015.06.002

Cavazzana, M., F. Touzot, D. Moshous, B. Neven, S. Blanche, and A. Fischer. 2014. Stem cell transplantation for primary immunodeficiencies: the European experience. *Curr. Opin. Allergy Clin. Immunol.* 14:516–520. http://dx.doi.org/10.1097/ACI.0000000000000119

Chambers, S.M., N.C. Boles, K.Y. Lin, M.P. Tierney, T.V. Bowman, S.B. Bradfute, A.J. Chen, A.A. Merchant, O. Sirin, D.C. Weksberg, et al. 2007. Hematopoietic fingerprints: an expression database of stem cells and their progeny. *Cell Stem Cell.* 1:578–591. http://dx.doi.org/10.1016/j.stem.2007.10.003

Chen, Y., X. Ma, M. Zhang, X. Wang, C. Wang, H. Wang, P. Guo, W. Yuan, K.L. Rudolph, Q. Zhan, and Z. Ju. 2014. Gadd45a regulates hematopoietic stem cell stress responses in mice. *Blood.* 123:851–862. http://dx.doi.org/10.1182/blood-2013-05-504084

Cheng, T., N. Rodrigues, H. Shen, Y. Yang, D. Dombkowski, M. Sykes, and D.T. Scadden. 2000. Hematopoietic stem cell quiescence maintained by p21cip1/waf1. *Science.* 287:1804–1808. http://dx.doi.org/10.1126/science.287.5459.1804

Cho, J., R. Yusuf, S. Kook, E. Attar, D. Lee, B. Park, T. Cheng, D.T. Scadden, and B.C. Lee. 2014. Purinergic $P2Y_{14}$ receptor modulates stress-induced hematopoietic stem/progenitor cell senescence. *J. Clin. Invest.* 124:3159–3171. http://dx.doi.org/10.1172/JCI61636

Cisternas, F.A., J.B. Vincent, S.W. Scherer, and P.N. Ray. 2003. Cloning and characterization of human CADPS and CADPS2, new members of the $Ca2^{+}$-dependent activator for secretion protein family. *Genomics.* 81:279–291. http://dx.doi.org/10.1016/S0888-7543(02)00040-X

Cohen, J.B., L.J. Burns, and V. Bachanova. 2015. Role of allogeneic stem cell transplantation in mantle cell lymphoma. *Eur. J. Haematol.* 94:290–297. http://dx.doi.org/http://dx.doi.org/10.1111/ejh.12442

Cutler, C., P. Multani, D. Robbins, H.T. Kim, T. Le, J. Hoggatt, L.M. Pelus, C. Desponts, Y.B. Chen, B. Rezner, et al. 2013. Prostaglandin-modulated umbilical cord blood hematopoietic stem cell transplantation. *Blood.* 122:3074–3081. http://dx.doi.org/10.1182/blood-2013-05-503177

Deneault, E., S. Cellot, A. Faubert, J.P. Laverdure, M. Fréchette, J. Chagraoui, N. Mayotte, M. Sauvageau, S.B. Ting, and G. Sauvageau. 2009. A functional screen to identify novel effectors of hematopoietic stem cell activity. *Cell.* 137:369–379. http://dx.doi.org/10.1016/j.cell.2009.03.026

Fares, I., J. Chagraoui, Y. Gareau, S. Gingras, R. Ruel, N. Mayotte, E. Csaszar, D.J. Knapp, P. Miller, M. Ngom, et al. 2014. Cord blood expansion. Pyrimidoindole derivatives are agonists of human hematopoietic stem cell self-renewal. *Science.* 345:1509–1512. http://dx.doi.org/10.1126/science.1256337

Fellmann, C., J. Zuber, K. McJunkin, K. Chang, C.D. Malone, R.A. Dickins, Q. Xu, M.O. Hengartner, S.J. Elledge, G.J. Hannon, and S.W. Lowe. 2011. Functional identification of optimized RNAi triggers using a massively parallel sensor assay. *Mol. Cell.* 41:733–746. http://dx.doi.org/10.1016/j.molcel.2011.02.008

Friedman, J.R., and K.H. Kaestner. 2006. The Foxa family of transcription factors in development and metabolism. *Cell. Mol. Life Sci.* 63:2317–2328. http://dx.doi.org/10.1007/s00018-006-6095-6

Geng, Y., Y. Dong, M. Yu, L. Zhang, X. Yan, J. Sun, L. Qiao, H. Geng, M. Nakajima, T. Furuichi, et al. 2011. Follistatin-like 1 (Fstl1) is a bone morphogenetic protein (BMP) 4 signaling antagonist in controlling mouse lung development. *Proc. Natl. Acad. Sci. USA.* 108:7058–7063. http://dx.doi.org/10.1073/pnas.1007293108

Gibbs, G.M., K. Roelants, and M.K. O'Bryan. 2008. The CAP superfamily: cysteine-rich secretory proteins, antigen 5, and pathogenesis-related 1 proteins--roles in reproduction, cancer, and immune defense. *Endocr. Rev.* 29:865–897. http://dx.doi.org/10.1210/er.2008-0032

Grant, C.E., T.L. Bailey, and W.S. Noble. 2011. FIMO: scanning for occurrences of a given motif. *Bioinformatics.* 27:1017–1018. http://dx.doi.org/10.1093/bioinformatics/btr064

Gruber, T.A., A. Larson Gedman, J. Zhang, C.S. Koss, S. Marada, H.Q. Ta, S.C. Chen, X. Su, S.K. Ogden, J. Dang, et al. 2012. An Inv(16)(p13.3q24.3)-encoded CBFA2T3-GLIS2 fusion protein defines an aggressive subtype of pediatric acute megakaryoblastic leukemia. *Cancer Cell.* 22:683–697. http://dx.doi.org/10.1016/j.ccr.2012.10.007

He, B., C. Chen, L. Teng, and K. Tan. 2014. Global view of enhancer-promoter interactome in human cells. *Proc. Natl. Acad. Sci. USA.* 111:E2191–E2199. http://dx.doi.org/10.1073/pnas.1320308111

Heng, T.S., and M.W. Painter. Immunological Genome Project Consortium. 2008. The Immunological Genome Project: networks of gene expression in immune cells. *Nat. Immunol.* 9:1091–1094. http://dx.doi.org/10.1038/ni1008-1091

Hoggatt, J., P. Singh, J. Sampath, and L.M. Pelus. 2009. Prostaglandin E2 enhances hematopoietic stem cell homing, survival, and proliferation. *Blood.* 113:5444–5455. http://dx.doi.org/10.1182/blood-2009-01-201335

Holmfeldt, P., J. Pardieck, A.C. Saulsberry, S.K. Nandakumar, D. Finkelstein, J.T. Gray, D.A. Persons, and S. McKinney-Freeman. 2013. Nfix is a novel regulator of murine hematopoietic stem and progenitor cell survival. *Blood.* 122:2987–2996. http://dx.doi.org/10.1182/blood-2013-04-493973

Hope, K.J., S. Cellot, S.B. Ting, T. MacRae, N. Mayotte, N.N. Iscove, and G. Sauvageau. 2010. An RNAi screen identifies Msi2 and Prox1 as having opposite roles in the regulation of hematopoietic stem cell activity. *Cell Stem Cell.* 7:101–113. http://dx.doi.org/10.1016/j.stem.2010.06.007

Ionescu, A., E. Kozhemyakina, C. Nicolae, K.H. Kaestner, B.R. Olsen, and A.B. Lassar. 2012. FoxA family members are crucial regulators of the hypertrophic chondrocyte differentiation program. *Dev. Cell.* 22:927–939. http://dx.doi.org/10.1016/j.devcel.2012.03.011

Ito, K., A. Hirao, F. Arai, K. Takubo, S. Matsuoka, K. Miyamoto, M. Ohmura, K. Naka, K. Hosokawa, Y. Ikeda, and T. Suda. 2006. Reactive oxygen species act through p38 MAPK to limit the lifespan of hematopoietic stem cells. *Nat. Med.* 12:446–451. http://dx.doi.org/10.1038/nm1388

Jang, Y.Y., and S.J. Sharkis. 2007. A low level of reactive oxygen species selects for primitive hematopoietic stem cells that may reside in the low-oxygenic niche. *Blood.* 110:3056–3063. http://dx.doi.org/10.1182/blood-2007-05-087759

Kuroiwa, M., C. Oneyama, S. Nada, and M. Okada. 2011. The guanine nucleotide exchange factor Arhgef5 plays crucial roles in Src-induced podosome formation. *J. Cell Sci.* 124:1726–1738. http://dx.doi.org/10.1242/jcs.080291

Lara-Astiaso, D., A. Weiner, E. Lorenzo-Vivas, I. Zaretsky, D.A. Jaitin, E. David, H. Keren-Shaul, A. Mildner, D. Winter, S. Jung, et al. 2014. Immunogenetics. Chromatin state dynamics during blood formation. *Science.* 345:943–949. http://dx.doi.org/10.1126/science.1256271

Ma, H., S. Mallampati, Y. Lu, B. Sun, E. Wang, X. Leng, Y. Gong, H. Shen, C.C. Yin, D. Jones, et al. 2014. The Sox4/Tcf7l1 axis promotes progression of BCR-ABL-positive acute lymphoblastic leukemia. *Haematologica.* 99:1591–1598. http://dx.doi.org/10.3324/haematol.2014.104695

Masetti, R., M. Pigazzi, M. Togni, A. Astolfi, V. Indio, E. Manara, R. Casadio, A. Pession, G. Basso, and F. Locatelli. 2013. CBFA2T3-GLIS2 fusion transcript is a novel common feature in pediatric, cytogenetically normal AML, not restricted to FAB M7 subtype. *Blood.* 121:3469–3472. http://dx.doi.org/10.1182/blood-2012-11-469825

Matsubara, A., A. Iwama, S. Yamazaki, C. Furuta, R. Hirasawa, Y. Morita, M. Osawa, T. Motohashi, K. Eto, H. Ema, et al. 2005. Endomucin, a CD34-like sialomucin, marks hematopoietic stem cells throughout development. *J. Exp. Med.* 202:1483–1492. http://dx.doi.org/10.1084/jem.20051325

McKinney-Freeman, S., P. Cahan, H. Li, S.A. Lacadie, H.T. Huang, M. Curran, S. Loewer, O. Naveiras, K.L. Kathrein, M. Konantz, et al. 2012. The transcriptional landscape of hematopoietic stem cell ontogeny. *Cell Stem Cell.* 11:701–714. http://dx.doi.org/10.1016/j.stem.2012.07.018

Moser, E., J. Kargl, J.L. Whistler, M. Waldhoer, and P. Tschische. 2010. G protein-coupled receptor-associated sorting protein 1 regulates the postendocytic sorting of seven-transmembrane-spanning G protein-coupled receptors. *Pharmacology.* 86:22–29. http://dx.doi.org/10.1159/000314161

Niesmann, K., D. Breuer, J. Brockhaus, G. Born, I. Wolff, C. Reissner, M.W. Kilimann, A. Rohlmann, and M. Missler. 2011. Dendritic spine formation and synaptic function require neurobeachin. *Nat. Commun.* 2:557. http://dx.doi.org/10.1038/ncomms1565

Rao, T.N., J. Marks-Bluth, J. Sullivan, M.K. Gupta, V. Chandrakanthan, S.R. Fitch, K. Ottersbach, Y.C. Jang, X. Piao, R.N. Kulkarni, et al. 2015. High-level Gpr56 expression is dispensable for the maintenance and function of hematopoietic stem and progenitor cells in mice. *Stem Cell Res. (Amst.).* 14:307–322. http://dx.doi.org/10.1016/j.scr.2015.02.001

Rossi, L., V. Salvestrini, D. Ferrari, F. Di Virgilio, and R.M. Lemoli. 2012. The sixth sense: hematopoietic stem cells detect danger through purinergic signaling. *Blood.* 120:2365–2375. http://dx.doi.org/10.1182/blood-2012-04-422378

Saito, Y., K. Kaneda, A. Suekane, E. Ichihara, S. Nakahata, N. Yamakawa, K. Nagai, N. Mizuno, K. Kogawa, I. Miura, et al. 2013. Maintenance of the hematopoietic stem cell pool in bone marrow niches by EVI1-regulated GPR56. *Leukemia.* 27:1637–1649. http://dx.doi.org/10.1038/leu.2013.75

Singer, K., R. Luo, S.J. Jeong, and X. Piao. 2013. GPR56 and the developing cerebral cortex: cells, matrix, and neuronal migration. *Mol. Neurobiol.* 47:186–196. http://dx.doi.org/10.1007/s12035-012-8343-0

Solaimani Kartalaei, P., T. Yamada-Inagawa, C.S. Vink, E. de Pater, R. van der Linden, J. Marks-Bluth, A. van der Sloot, M. van den Hout, T. Yokomizo, M.L. van Schaick-Solernó, et al. 2015. Whole-transcriptome analysis of endothelial to hematopoietic stem cell transition reveals a requirement for Gpr56 in HSC generation. *J. Exp. Med.* 212:93–106. http://dx.doi.org/10.1084/jem.20140767

Sun, J., A. Ramos, B. Chapman, J.B. Johnnidis, L. Le, Y.J. Ho, A. Klein, O. Hofmann, and F.D. Camargo. 2014. Clonal dynamics of native haematopoiesis. *Nature.* 514:322–327. http://dx.doi.org/10.1038/nature13824

Talano, J.A., and M.S. Cairo. 2015. Hematopoietic stem cell transplantation for sickle cell disease: state of the science. *Eur. J. Haematol.* 94:391–399. http://dx.doi.org/http://dx.doi.org/10.1111/ejh.12447

Taniguchi Ishikawa, E., D. Gonzalez-Nieto, G. Ghiaur, S.K. Dunn, A.M. Ficker, B. Murali, M. Madhu, D.E. Gutstein, G.I. Fishman, L.C. Barrio, and J.A. Cancelas. 2012. Connexin-43 prevents hematopoietic stem cell senescence through transfer of reactive oxygen species to bone marrow stromal cells. *Proc. Natl. Acad. Sci. USA.* 109:9071–9076. http://dx.doi.org/10.1073/pnas.1120358109

Tothova, Z., R. Kollipara, B.J. Huntly, B.H. Lee, D.H. Castrillon, D.E. Cullen, E.P. McDowell, S. Lazo-Kallanian, I.R. Williams, C. Sears, et al. 2007. FoxOs are critical mediators of hematopoietic stem cell resistance to physiologic oxidative stress. *Cell.* 128:325–339. http://dx.doi.org/10.1016/j.cell.2007.01.003

Urrutia, R. 2003. KRAB-containing zinc-finger repressor proteins. *Genome Biol.* 4:231. http://dx.doi.org/10.1186/gb-2003-4-10-231

Walasek, M.A., R. van Os, and G. de Haan. 2012. Hematopoietic stem cell expansion: challenges and opportunities. *Ann. N.Y. Acad. Sci.* 1266:138–150. http://dx.doi.org/10.1111/j.1749-6632.2012.06549.x

Wei, K., V. Serpooshan, C. Hurtado, M. Diez-Cuñado, M. Zhao, S. Maruyama, W. Zhu, G. Fajardo, M. Noseda, K. Nakamura, et al. 2015. Epicardial FSTL1 reconstitution regenerates the adult mammalian heart. *Nature.* 525:479–485. http://dx.doi.org/10.1038/nature15372

Weirauch, M.T., A. Yang, M. Albu, A.G. Cote, A. Montenegro-Montero, P. Drewe, H.S. Najafabadi, S.A. Lambert, I. Mann, K. Cook, et al. 2014. Determination and inference of eukaryotic transcription factor sequence specificity. *Cell.* 158:1431–1443. http://dx.doi.org/10.1016/j.cell.2014.08.009

Wilson, A., M.J. Murphy, T. Oskarsson, K. Kaloulis, M.D. Bettess, G.M. Oser, A.C. Pasche, C. Knabenhans, H.R. Macdonald, and A. Trumpp. 2004. c-Myc controls the balance between hematopoietic stem cell self-renewal and differentiation. *Genes Dev.* 18:2747–2763. http://dx.doi.org/10.1101/gad.313104

Xu, L., V. Panel, X. Ma, C. Du, L. Hugendubler, O. Gavrilova, A. Liu, T. McLaughlin, K.H. Kaestner, and E. Mueller. 2013. The winged helix transcription factor Foxa3 regulates adipocyte differentiation and depot-selective fat tissue expansion. *Mol. Cell. Biol.* 33:3392–3399. http://dx.doi.org/10.1128/MCB.00244-13

Zhang, H., M. Alberich-Jorda, G. Amabile, H. Yang, P.B. Staber, A. Di Ruscio, R.S. Welner, A. Ebralidze, J. Zhang, E. Levantini, et al. 2013. Sox4 is a key oncogenic target in C/EBPα mutant acute myeloid leukemia. *Cancer Cell.* 24:575–588. http://dx.doi.org/10.1016/j.ccr.2013.09.018

Zhang, Y., E. Diaz-Flores, G. Li, Z. Wang, Z. Kang, E. Haviernikova, S. Rowe, C.K. Qu, W. Tse, K.M. Shannon, and K.D. Bunting. 2007. Abnormal hematopoiesis in Gab2 mutant mice. *Blood.* 110:116–124. http://dx.doi.org/10.1182/blood-2006-11-060707

Zhao, C., J. Blum, A. Chen, H.Y. Kwon, S.H. Jung, J.M. Cook, A. Lagoo, and T. Reya. 2007. Loss of β-catenin impairs the renewal of normal and CML stem cells in vivo. *Cancer Cell.* 12:528–541. http://dx.doi.org/10.1016/j.ccr.2007.11.003

Zhong, X.Y., B. Zhang, R. Asadollahi, S.H. Low, and W. Holzgreve. 2010. Umbilical cord blood stem cells: what to expect. *Ann. N.Y. Acad. Sci.* 1205:17–22. http://dx.doi.org/10.1111/j.1749-6632.2010.05659.x